NTNU

Norwegian University of
Science and Technology

Performance of Stability Indicators based on Phasor Measurements

Pascal Muhirwa

Master of Science in Electric Power Engineering
Submission date: June 2018
Supervisor: Kjetil Uhlen, IEL
Co-supervisor: Dinh Thuc Duong, IEL

Norwegian University of Science and Technology
Department of Electric Power Engineering

Abstract

The development of Wide Area Measurements (WAMS) is growing with the increasing usage of Phasor Measurements Units(PMU) in power systems. Its introduction gives power system operators greater observability, as PMUs can measure the voltage angle and magnitude in real time (up to 50/60 recordings per second), with the help of GPS technology. Given better situational awareness, system operators gain a higher chance of preventing unstable or insecure operation of the power system. The applications of PMU measurements are many, on the subject of power system stability the availability of using PMU measurements makes it possible to estimate system modal characteristics directly from the measurements. System identification and signal processing method has in the last decades been studied and customized for power system application, particularity to estimate modal properties in power systems.

The objective of this thesis is to assess the performance of two algorithms which are commonly used in the structure and civil engineering for modal estimation. The two methods investigated in this report, are the Natural Excitation Technique used in conjunction with Eigensystem Realization Algorithm (NExT-ERA) and Multivariate Auto-regressive model(MAR). The NexT-ERA is a twofold algorithm. The first algorithm, The Natural Excitation Technique, can estimate impulse responses of power systems by calculating cross-correlation functions between measurement. The second algorithm, Eigensystem Realization Algorithm, uses the impulse responses calculated with NExT to estimate a state-space model of the power system. From the state matrix, the eigenvalues which describes the dynamic of the system can thus be extracted. Multivariate Auto-regressive model is an extension of the Auto-regressive model which uses multiple signals to fit into the model. The modal properties can be calculated by the parameters of the MAR model by eigendecomposition.

This thesis shows that the methods can estimate the electromechanical modes, which correspond to low-frequency oscillations that are excited by continuously varying loads. The performance of the methods is investigated by comparing prior knowledge of the modal properties from a synthetic signal, simulation model and the Nordic power grid with estimated values. The evaluation of the performance of the methods is based on the consistency of the estimation for different window length and model order. The evaluated results are designated to give the reader input on how NExT-ERA and MAR perform as a stability indicator for power systems. Which may motivate the reader to implement and study the method further with the intent to create an application for real-time and off-line modal identification.

Sammendrag

Utviklingen av kontroll og overvåkingssystemet knyttet til bruken av vektormålere (PMU) i kraftsystemet, har ført til utvikling av det langt omfattende overvåkingssystem Wide Area Measurement System (WAMS). Dens innføring gir operatører i kraftsystemet større observasjon av dynamikken i kraftsystemet, da vektromålere kan måle opptil 50/60 opptak per sekund og måle synkront ved hjelp av GPS-teknologi. Gitt bedre informasjon om forløpet til systemets dynamikk, har systemoperatørene større sjanse til å forhindre kraftsystemet til å driftes forsyningsstridig.

Applikasjonene til vektormålere er mange. Med hensyn til stabilitet i kraftnettet, gjør tilgjengeligheten av å bruke målinger fra vektormålere det mulig å estimere systemets modale egenskaper direkte fra målinger i nettet. Metoder og teknikk fra systemidentifikasjon og signalbehandling har i de siste tiårene blitt studert og tilpasset til bruk i sammenheng med identifikasjon av modale egenskaper knyttet til kraftsystemer. Målet i denne oppgaven har vært å vurdere hvordan to algoritmer som ofte brukes i konstruksjon og bygningsteknikk for modal estimering, fungerer i bruk av estimering av lavfrekvente modi i kraftsystem ved hjelp av vektormålere. De to metodene som undersøkes i denne rapporten, er The Natural Excitation Technique som brukes i sammenheng med Eigensystem Realization Algorithm (NExT-ERA), og Multivariate Auto-regressive modell (MAR). NexT-ERA er en todelt algoritme. Den første algoritmen, The Natural Excitation Technique, kan estimere impulsresponser av kraftsystemer ved å beregne krysskorrelasjonsfunksjoner mellom målingene fra vektormålere. Den andre algoritmen, Eigensystem Realization Algorithm, bruker impulsresponsene beregnet med NExT for å estimere en tilstandsmodell av kraftsystemet. Slik at, fra tilstandsmatrisen så kan egenverdiene som beskriver systemets dynamikk, beregnes.

Multivariate Auto-regressive modellen er en forlengelse av den Auto-regressive modellen som bruker flere målesignaler til å tilpasse den Auto-Regressive modellen. De modale egenskapene kan beregnes av parametrene til MAR-modellen ved dekomponering av koeffisient matrisen.

Denne oppgaven viser at metodene kan estimere de elektromekaniske modiene, som eksiteres av kontinuerlig varierende last. Funksjonaliteten til metodene undersøkes ved å sammenligne forhåndsberegnet modi fra et syntetisk signal, simuleringsmodell av nordiske kraftsystemet og det reelle nordiske kraftnettet. De evaluerte resultatene er ment å gi leseren et overblikk om hvordan NExT-ERA og MAR fungerer som stabilitetsindikator for kraftsystem.

Preface

This thesis is submitted to the Faculty of Information Technology, Mathematics and Electrical Engineering (IE) as a requirement of fulfilling the master studies in Electrical Power Engineering at the Norwegian University of Science and Technology.

I would like to thank my supervisor, Professor Kjetil Uhlen, for his guidance and insights during the last two semesters. I would also thank my co-supervisor, Dinh Thuc Duong, who is a Ph.D. candidate and has been very helpful in the process. And lastly, I would like to thank my fellow students, friends, and family for all the support throughout all the years of studies.

Contents

List of Figures

List of Tables

Abbreviations

ERA Eigensystem Realization Algorithm. v

GPS Global Positioning System. v

LPM Linear Prediction Method. v

MAR Multivariate Auto-Regressive Model. v

NExT Natural Excitation Technique. v

NTNU Norwegian University of Science and Technology. v

PDC Phasor Data Concentrator. v

PMU Phasor Measurement Unit. v

SBC Schwarz's Bayesian Criterion. v

SCADA Supervisory Control and Data Acquisition. v

SNR Singal to Noise Ratio. v

WACS Wide Area Control Systems. v

WAMS Wide Area Measurement Systems. v

Chapter 1

Introduction

1.1 Background ant Motivation

Power systems are complex interconnected systems with the purpose of delivering electricity to consumers, at demand. Operating a power system is complex. Many requisites have to be met for the power system to meets its objective. One of the issues that threats the security of power system is the electromechanical oscillations. Electromechanical oscillations are inherent in power systems, and they stem from generators swinging relatively to one another or against a group of generators, due to continuously varying load in the system. The low damping in some of these oscillations is a limiting factor on the systems transmission capacity. In severe situations, they can grow and cause several outages, and in worst case blackouts[1],[2],[3].

To prevent the threat by electromechanical oscillation, the frequency of the oscillations and their corresponding damping ratio may be monitored with wide area measurement systems(WAMS). Damping ratio is a stability indicator on the systems ability to tackle oscillatory behavior. Monitoring the number of damping areas has, the system operators can take measures in early stages before a possible failure occurs due to electromechanical oscillation. Thus, power oscillation monitoring is essential, as it gives power system operators a situation awareness they can act upon.

Currently, the concept of wide area measurement system and control is being developed, tested and gradually implemented into control room application. Wide area measurement system is the utilization of system-wide information obtain by phasor measuring units, PMUs. A PMU is a unit that can measure synchronized current and voltage

phasors, which can measure up to 50/60 records per second. Utilizing multiple synchronized PMUs, dynamic information from dominant inter-area paths can be obtained and observed. These time-domain measurements have enabled the possibility for online modal identification.

Traditionally, the stability studies concerning oscillatory behavior in power systems are conducted off-line with extensive simulations. However, with the development of PMUs, there has been conducted many studies on estimation of modal properties in power system using signal processing and system identification techniques and algorithms. In this thesis, the capability of Natural Excitation Technique in conjunction with Eigensystem Realization Algorithm is investigated together with the method Multivariate Auto-regressive model. The objective is to evaluate their performance to estimate the oscillatory stability of a power system using PMU data.

The Natural Excitation Technique used in conjunction with Eigensystem Realization Algorithm (NExT-ERA) and Multivariate Auto-regressive (MAR) is common dynamic estimation methods used in the structure and civil engineer to estimate ambient responses. NExT-ERA algorithm consists of two different algorithms. The first algorithm, NExT, estimate the impulse response of the power system by utilizing cross-correlation functions between measurements from PMUs. The ERA algorithm is then used to identify a state-space model of the power system with the impulse responses. By, obtaining the state-space model, the modal properties can easily be calculated.

MAR is an extension of the Auto-regressive model which uses multiple signals to calculate the present value as a weighted linear sum of previous values. By fitting the time-series to a MAR model, the modal properties of the system can be obtained by eigenvalue decomposition. The method along with NExT-ERA has proven to be functional for estimating the electromechanical modes by [4],[5],[6],[7]. Therefore NTNU and the electrical power engineering faculty has sought out to gain experience of their performance.

1.2 Scope and Objective

The primary objective of the thesis is to show that NExT-ERA and MAR are capable of identifying the modal properties of low-frequency oscillation in power systems and examine their performance. Before the methods are tested on real PMU data, the algorithms are tested with a synthetic signal and generated PMU data by simulation from a test network. All the PMU data used are ambient data from the Norwegian power grid provided by the supervisor, Kjetil Uhlen together with a test network that is used to obtain simulated data. The NExT-ERA is implemented in MATLAB, while co-supervisor Dinh Thuc Duong provided the code for MAR in MATLAB.

1.3 Outline of Thesis

The thesis is organized into six chapters. First theoretical background on power system stability, signal processing and the algorithms to be examined are reviewed in chapter 2. The following chapter 3,4 and 5 investigate the performance of the methods with a synthetic signal, simulated PMU data and real PMU data respectively. Chapter 4 focuses on how the method responds to different noise levels. Chapter 5 focuses on how the model order and window length affect the estimation of modal properties with real PMU data. Chapter 6 summarize, discuss and conclude the findings.

Chapter 2

Background

The purpose of this chapter is to provide the reader, some of the background to understand the concepts and methods used in this report as well as establishing the basis for the report. The chapter presents the stability concept related to rotor angle stability and the concept of using wide area measurement system to control and identify the electromechanical modes as well as theory related to modal identification.

2.1 Phasor

The currents and voltage in the commercial power systems are alternating. They are represented as sine or cosine function with time. In the time domain, the voltages are mathematically described as:

$$v(t) = V_m cos(\omega t + \delta) \tag{2.1}$$

Where V_m is the amplitude of the sinusoidal wave, δ is the phase shift, ωt is the angular frequency which is defined as $2\pi f$, whereas f is the frequency. A similar representation can be made for currents.

A phasor is a sinusoidal waveform represented as a time-invariant vector, where its magnitude corresponds to the amplitude of the sinusoidal, and its angle is the angular separation between a reference time. The phasor representation is deduced by Euler's formula, by:

$$v(t) = V_m e^{j\delta} e^{jwt} = \sqrt{2}\underline{V} e^{jwt} \tag{2.2}$$

where

$$\underline{V} = V e^{j\delta} = V(cos\delta + jsin\delta) \tag{2.3}$$

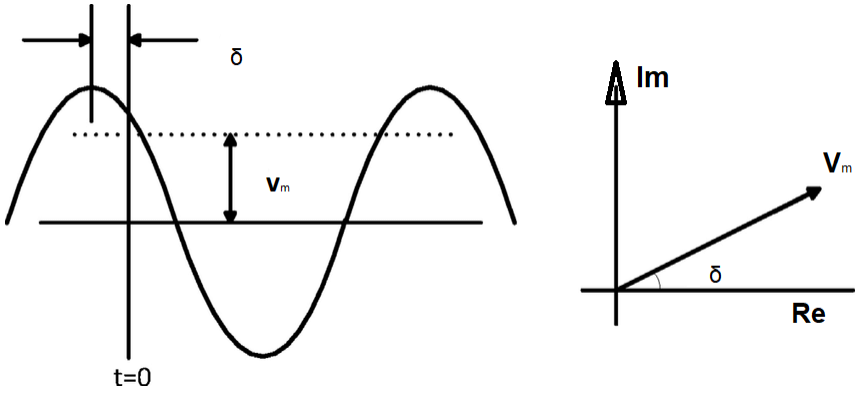

Figure 2.1: Phasor representation of voltage

Figure 2.1 shows a signal in a time-frame and the corresponding phasor of the signal projected into a complex plane. Let t_0 be the reference time, and peak be when the phase-shifted sinusoidal reaches its peak. When the reference frame and the phasor move at the same rate, the time-varying component $e^{j\omega t}$ can be dropped in 2.2. As a result, the vector becomes standing still. This allow the function to be presented as a phasor with only its magnitude and angle as an angular separation of the reference frame in the complex plane.

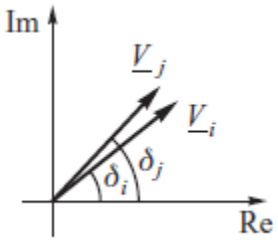

Figure 2.2: Voltage phasors in the complex plane

The state of a power system with n number of nodes can be determined by determining the voltage magnitudes and voltage angles in the system. Thus, to determine the system

state, one can measure the voltages and fit them into one common reference such that the relative voltage angles between each bus voltage do not change with time, like in figure 2.2. This enables the voltage phasors to be measured and calculated into the reference frame and thus determine the state of the system.

2.2 Phasor Measuring Unit

A phasor measurement unit is a time synchronized measurement device that measures voltage and current signals represented as phasor and the frequency. Measuring the voltage and currents as phasors makes it possible to place them into a common reference frame directly. By using GPS technology to time stamp, the measured phasors makes it possible to measure voltages and currents at a different location simultaneously accurately. Subsequently, the relative phase angles between the nodes in the network can be determined directly, which enables to calculate the powers of the power system fast[2].

2.3 Wide Area Measurement and Control System

Wide Area Measurement Systems (WAMS) and Wide Area Control Systems(WACS) are data acquisition and control systems which use synchronized phasor measurement data to monitor power system dynamics. By monitoring, possible weaknesses(WAMS) in the system can be identified, and corresponding countermeasures can be developed[2].

The current Energy Management Systems use Supervisory Control and Data Acquisition(SCADA) as a tool for data acquisition. The SCADA system is not able to coordinate the measurements synchronously, and it has a slower rate than PMU, leaving out most of the dynamics of power systems. SCADA record data every 2-10 second, while PMU record 50/60 records per second. For this reason, the introduction to WAMS and WACS has been paid much attention and is tediously researched. An example of a three-layered WAMS structure is shown in figure 2.3. The PMUs deployed in the figure are time stamped with a GPS receiver. The data acquired measured from PMUs are forwarded to phasor data concentrator(PDC) which supply data for system monitoring, protection and control. The layer in the middle combine the measurements from different areas, while the top layer of PDC's combine all the information and forward it to the control center.

The concept has been widely discussed over the past decades, and its entry to the power system is a natural response to the way power system is operated. The electric power utilities has to optimal run the power systems due to economic restraints and technical restraints [8],[9],[4]. One of the main concerns is the limited transfer capability between areas. The limiting factor is due to high probability of oscillations due to low damping. The utility company cannot fully exploit the thermal capability of the transmission lines. As a consequence, the power systems are running close to their transfer capabilities which could lead to unforeseen contingencies. Thus, it becomes necessary to be able to monitor and observe the power system also increase the power transfer capabilities.

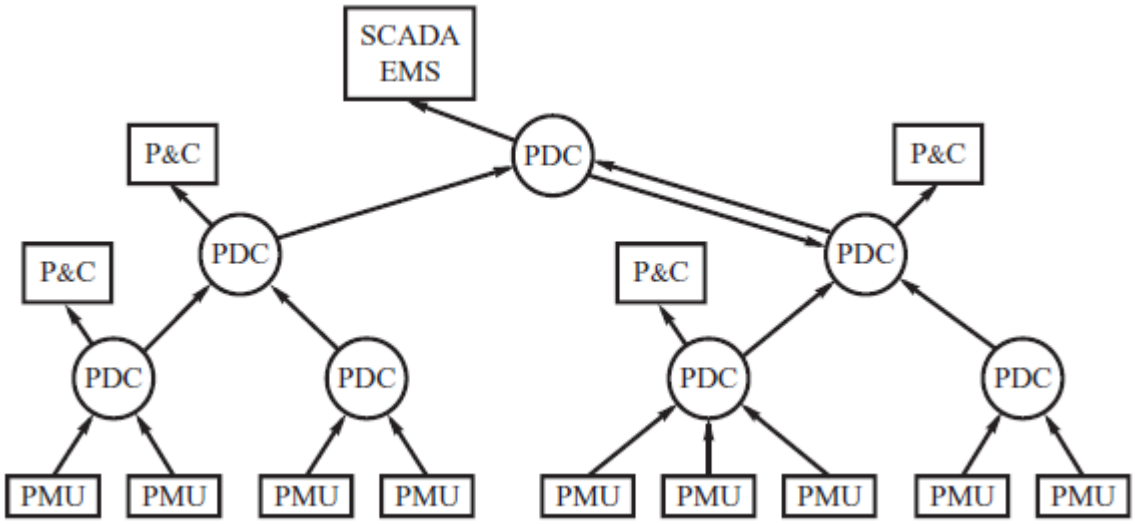

Figure 2.3: Example of structure of Wide Area Measurements

The current Energy Management Systems use Supervisory Control and Data Acquisition(SCADA) as a tool for data acquisition. The SCADA system is not able to coordinate the measurements synchronously, and it has slower rate than PMU, leaving out most of the dynamics of power systems. SCADA record between 2-10 per second, while PMU record 50/60. For this reason, the introduction to WAMS and WACS has been paid much attention and is tediously researched.

2.4 Power System Stability

Power systems are complex interconnected networks with the purpose of delivering electrical power to consumers at demand. Due to its inherent non-linear nature and dynamic interaction between power system elements, the challenges associated with a power system correspond to the ability to deliver power and keep the system elements intact following any disturbance. The response of the power system is what defines its stability. In definition, the stability of a power system is defined as the ability to remain in a state of equilibrium under normal operation and the ability to regain a satisfactory equilibrium point after being subjected to a disturbance. A power system response to a disturbance involves many of the system elements. Following a disturbance some elements may actuate other few elements, while others actuate a wide range of elements, and some the whole system. Depending on the elements that upset the power system stability after a disturbance, the stability problem is categorized by rotor angle, voltage and frequency stability.

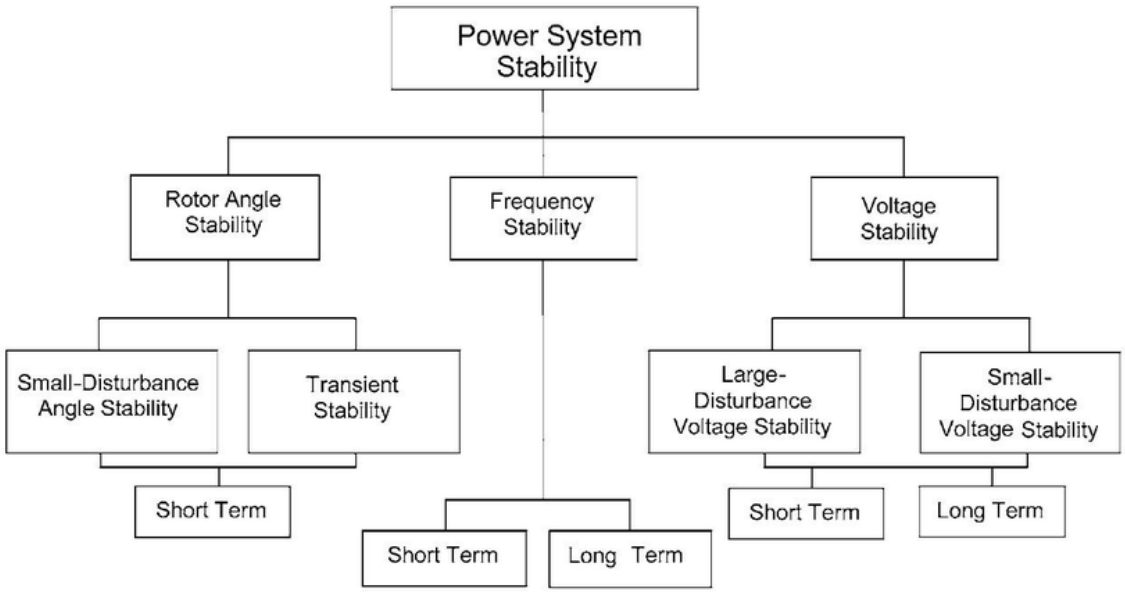

Figure 2.4: Classification of power system stability

Depending on type, size and time span of disturbance, the stability is classified as in figure 2.4. The rotor angle stability is defined as the ability of synchronous machines in power systems to remain in synchronism following a disturbance. Frequency stability is defined as the ability of the system to keep a steady state frequency following a disturbance that upset the balance of generation and load. While Voltage stability is

defined as the ability of the power system to keep a steady state voltage following a disturbance.

2.4.1 Rotor angle stability

The rotor angle stability is associated with the study of rotor speed interactions with electromagnetic changes, which are referred to as electromechanical dynamics[2]. To understand it, the manner of how generator output power as a function of rotor angle must be understood first.

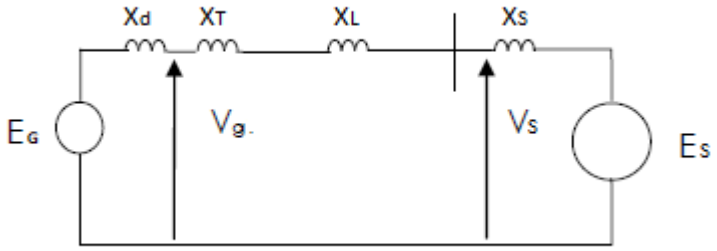

(a) The equivalent diagram of figure 2.5b.

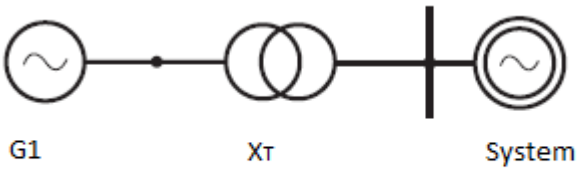

(b) A generator G_1 connected to groups of generators represented as G_S through a transmission line and transformer. G_S is assumed to have the same characteristics as an infinity bus.

Let us consider the two bus system in figure 2.5b with G_1 connected to other groups of generator represented by G_S with the same characteristics as an infinity bus. G_1 is connected to G_S through a transformer X_T and a transmission line X_L.

E_G is the internal emf behind the generator reactance X_d, and X_s is the reactance of G_s in which E_S is behind. In the simplest form, the power transfer from G_1 to the rest of the system presented by G_S is given by:

$$P = \frac{E_G V_s}{X} sin\delta \tag{2.4}$$

$$Q = \frac{E_G V_S}{X} cos\delta - \frac{V_S^2}{X} \tag{2.5}$$

where

$X = X_d + X_T + X_L$ is the transfer reactance and $\delta = \delta_G + \delta_L + \delta_S$ is referred to as the rotor angle and it is the angular separation between the generator rotor G_1 and system generator rotor G_S. Since voltages must be kept within a small percentage of limit, they are assumed constant, and hence changes in active power correspond to the sinusoidal variation of the rotor angle. An active power vs rotor angle relationship is plotted in figure 2.6 for the simplified and idealized model, where P_E is the electrical power from generator G_1 and P_M is the mechanical power. As it can be seen from the figure, the power transfer depends on the rotor angle, when it is zero there is no transfer. The power transfer has a certain maximum limit, in this case, when the rotor angle equals 90 degrees and further increases from the maximum point result in a decrease of power transfer.

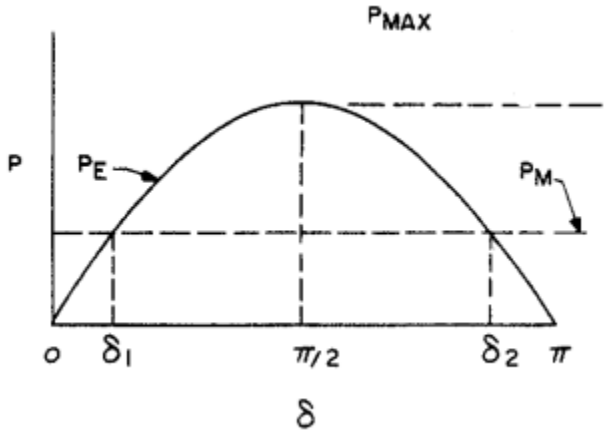

Figure 2.6: Power vs rotor angle relationship

Swing equation

The power system presented in figure 2.5b is considered in equilibrium (steady state) stable when each generators electrical air gap power (electrical power) is equal and opposite to its turbine shaft power (mechanical power), and the speed is constant. This behavior is according to Newton's law of motion described by equation 2.6 called the swing equation.

$$M\frac{d^2\delta}{dt^2} = P_m - P_e - D\frac{d\delta}{dt} = P_{acc} \tag{2.6}$$

Where P_m is the turbine shaft power, P_e is the air gap power, and D is the damping coefficient. While M is the inertia coefficient and δ is the rotor angle.

When a disturbance occurs, a shift in power balance results in the system moving away from the equilibrium point. This makes according to the swing equation the rotors of the machines in power system to accelerate or decelerate. If for instance, a disturbance cause generator G_1 angular speed to run faster, its rotor angle will advance relative to the groups of generator represented by G_S. This result in that part of the G_S load is shifted to G_1, which correspond to increase in power according to the power vs. rotor angle relationship. While G_S power is reduced. This tends to reduce the speed difference, and hence the angle difference. If the faster-running machine rotor angle advance beyond a limit, the power transfer capability reduces, which in turn increase the angular separation between the generators and leads to a machine to lose synchronism with the rest of the system, in this instance, G_1 fall out of step with system G_S.

Synchronizing torque and damping torque

Following a disturbance, the changes in the electrical torque are described by a synchronizing torque and damping torque. The synchronizing torque is component corresponding to torque change in phase with rotor angle, and this torque can be deduced from $P_e(\delta)$ in swing equation. Lack of sufficient synchronizing torque results in instability in the form of periodic shifts in rotor angle. While damping torque corresponds to the term $D\frac{d\delta}{dt}$ in swing equation 2.6. The damping torque is associated with speed changes, and lack of damping torque result in instability in the form of oscillations.

2.4.2 Small-signal stability

Analysis of stability associated with rotor angle stability is divided into small-signal and transient stability. Small signal stability is the ability of a power system to maintain the system synchronized during small disturbances. Transient stability is the ability of a power system to maintain synchronism after being subjected to large disturbances. Only the concept of small signal stability is elaborated in this report.

Small disturbances instability can occur in either due to lack of sufficient synchronizing torque or damping torque. In today's power systems, instabilities associated with lack of sufficient synchronizing torque are almost non-existent since nowadays the generators are equipped with automatic voltage regulators. Most problems correspond to lack of sufficient damping of oscillations[3]. These oscillations are referred to as electromechanical oscillations.

Electromechanical oscillations can occur either locally or globally. The local problem is referred to a single generator rotor oscillations against the rest of its system and is called local plant oscillation mode. The generators in local plant oscillations swing at 1.0 to 2.0 Hz against its systems. Global problems involve groups of generators in an area oscillating against other groups of generators in another area and are known as inter-area oscillation mode. The oscillations are usually between 0.1 and 1.0 Hz.

Other modes associated with rotor angle stability are control-modes which involve poorly tuned controllers that contribute to reducing the damping torque. Another mode is the Torsional mode which is a reference to generator and turbine shaft system rotational components. Its instability may be caused by excitation controller, speed governor control or series-capacitor compensated line controllers.

2.5 Signal Processing and Modal Identification

One of many applications to WAMS is the monitoring of low-frequency oscillations. Monitoring the low-frequency oscillations on-line with synchronized PMUs make it possible to detect poorly damped oscillations in real-time. To estimate the modal components of the inter-area oscillations numerical algorithms are often used. Small signal stability analysis using modal identification algorithms originate from signal processing and system identification methods, but have in the last decades had a growing application and customization to the estimation of modal components in power systems.

There exist two approaches for identifying modal properties in small signal stability analysis. One approach is based on linear analysis using eigenvalue analysis techniques. While the second approach is based on processing time domain data and is the one referred to as modal identification[7], using system identification techniques.

Linear analysis has proven to give accurate stability characteristics(frequency, damping and mode shapes) for the given operating point. The steps in this approach are performed by obtaining the linearized state matrix, which is obtained by linearization of the non-linear differential equations describing the system dynamics(swing equation). This is followed up by an eigenvalue analysis which gives the characteristics of the system by the eigenvalues obtained. This approach is desirable as it enables a detailed model of the power system and by using numerical methods, accurate dynamic information is obtainable for a given operating point. However, the limitation of this method is that it can only obtain dynamics for a given operating point and only a small number of modes can be obtained for large power systems.

Modal identification is the process of determining modal components by measured data using system identification methods. The modal identification is based on signal processing techniques and has had a growing application to power system over the last decades. These methods are an alternative approach to obtain dynamic characteristics when it is not possible or preferable to use linearized power system equations. The essence of system identification is to replicate a system with an equivalent model based on observed data. A model can be a mathematical description of the system which describes its variables and relationship of the system variables. In the instance of modal estimation of a power system, many of the models used contain variables with the dynamical properties of the system, determining those variable allow the user to obtain valuable information about power system dynamics. Furthermore, the disadvantage with the identification methods is that well-damped modes and dynamics embedded in signal noise are difficult to detect. Also, the selection of model order is a challenge and

practical issue[7].

The methods and algorithms developed for modal identification in power system are classified based on power system response. There are broadly two responses. Ambient and transient(ringdown). A response is considered an ambient response when there are random variations in the system excited by small amplitude variation, such as load variations. Whereas a transient is substantially larger in amplitude, which is often caused by a contingency or switch.

2.5.1 Parametric vs Non-parametric Methods

In system identification, the analysis methods are classified either as a parametric or non-parametric method. The most common approach is to use parametric methods which consist of fitting a set of observed data to a model with many unknown parameters. Estimating the parameters provide the model with the best fit to the observed data [10],[11]. The advantage of parametric methods is the high amount of data reduction, by going from a large set of measurement data to a small set of parameters. However, one of the main difficulties of the parametric method is to choose the model structure.

The other method is non-parametric, which is an estimation without using a predefined model with unknown parameters. The non-parametric method uses the observed data directly to estimate the frequency and impulse response for the system. In many instances, the non-parametric method is used to verify the parametric methods. For example, using the spectral density of a signal help discover if the signal contains the frequency of interest.

2.5.2 Analysis of Ambient Measurements

The random load variations that continuously probe the power systems is the cause for the ambient oscillations, and they are conceptualized as unknown inputs noise. When recording the ambient oscillations, these noises are translated to the records. An Ambient analysis in power system refers to the estimation of mode shapes when the primary excitation is the random variations [10],[4]. Ambient analysis can be conducted either in frequency or time domain. Time-domain algorithms perform the estimation on the sampled data set, while frequency-based methods need to to use spectral density functions. However, before estimating the modes, it is useful to perform a spectral

density estimation using, for example, Welch's periodogram functions. By doing so, the user can be aware of which frequencies are dominant in the signals. The dominant modes correspond to the peaks in the spectral periodogram.

The figure 2.7 shows an example of Welch's power spectral density estimate. The signal used is the synthetic signal in 2.7 with a sampling frequency of 100 Hz.

$$\begin{aligned} y(n) =& 50cos(2\pi 1.68n - 0.2\pi) * e^{-0.1n} + 5cos(2\pi 2.0n \\ &+ 0.1\pi)e^{0.2n} + 12cos(2\pi 0.69n - 0.3\pi)e^{-0.5n} \end{aligned} \tag{2.7}$$

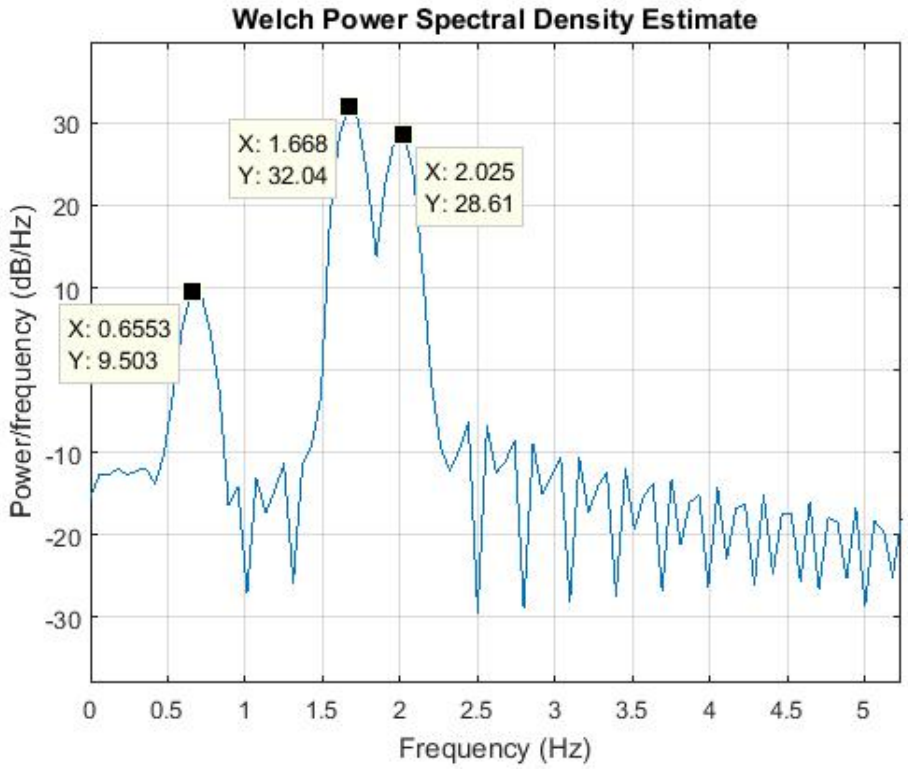

Figure 2.7: Example of Welch's power spectral density estimate

From the figure 2.7 it can be seen that the frequency peaks correspond well with the frequency of the signal in 2.7. Using this as an additional tool in ambient analysis can help validate the estimation of the modes. Other periodogram using Fourier transformation can be found in signal processing literature [12],[11].

2.6 Theoretical Background of Modal Estimation Methods

The goal of the following sections is to introduce the theoretical background for the linearization method modal analysis as well as modal identification method MAR, NExT-ERA and Prony algorithms.

2.6.1 Modal Analysis - Linear Analysis

A power system is described by a set of nonlinear equations and can be written in the state space form of equation 2.8. Where x is a vector of state variables, and A is the state matrix. A nonlinear system can be linearized around an operating point. For a power system this is only valid for small deviations from the operating point, hence small disturbances.

$$\dot{\mathbf{x}} = \mathbf{A}\mathbf{x} \tag{2.8}$$

Equation 2.8 has the solution:

$$\mathbf{x(t)} = \mathbf{x}\mathbf{e}^{\mathbf{At}} = \mathbf{x_1}\mathbf{e}^{\lambda_1 \mathbf{t}} + \mathbf{x_2}\mathbf{e}^{\lambda_2 \mathbf{t}} + \cdots + \mathbf{x_n}\mathbf{e}^{\lambda_n \mathbf{t}} \tag{2.9}$$

The state variables x can be transformed into a new state variables $\mathbf{z}$:

$$\mathbf{x} = W\mathbf{z} \tag{2.10}$$

Substituting 2.10 into state space equation 2.8 result in:

$$\dot{\mathbf{z}} = \mathbf{W}^{-\mathbf{1}}\mathbf{A}\mathbf{W}\mathbf{z} \tag{2.11}$$

$$\dot{\mathbf{z}} = \mathbf{\Lambda z} \tag{2.12}$$

Where W is the right eigenvectors of state matrix A and is referred to as the modal matrix, Λ is the modal form of the state matrix, and z is the modal variables also referred to as modes. The differential equations have the solution:

$$\mathbf{z(t)} = \mathbf{e^{\Lambda t} z_0} \tag{2.13}$$

Whereas z_0 is the initial condition. The set of vector solution can be expressed as a scalar:

$$z_i(t) = e^{\lambda_i t} z_{i0} \qquad\qquad i = 0, 1, 2....n \tag{2.14}$$

The effect of modal transformation is that the state matrix A, which in general is non-diagonal is transformed into a diagonal matrix Λ such that the state equations become decoupled. The modal variables in 2.14 are the solution of the decoupled state equations. The modal variables hold information about the response of the state variable from each of its state equation. The state variable can be expressed as a linear combination of modal variables by transforming back using 2.10:

$$\mathbf{x(t)} = \mathbf{W e^{\Lambda t} z_0} \tag{2.15}$$

which implies that

$$x_k = w_{k1} z_{10} e^{\lambda_1 t} + w_{k2} z_{20} e^{\lambda_2 t} + \cdots + w_{ki} z_{i0} e^{\lambda_i t} \tag{2.16}$$

where the initial conditions z_0 can be expressed as $\mathbf{z_0} = \mathbf{U x_0}$. U is the left eigenvectors and is the inverse of the right eigenvectors since they are orthogonal. In the more

compact form we get:

$$x_k = w_{k1}z_1 + w_{k2}z_2 + \cdots + w_{ki}z_i \tag{2.17}$$

The above equation represents the time response of free motion in terms of eigenvalues and right and left eigenvector. The right eigenvector carries information about the observability of the modal variables for an individual state variable. If the eigenvectors are normalized, then the right eigenvector w_{ki} determines the share of involvement of modal variable z_i in the state variable x_k in terms of magnitude and phase. This share of involvement is referred to as the mode shape. The left eigenvector carries information about the controllability of modal variables for an individual state variable. Similar to right eigenvectors, if the eigenvectors are normalized, then the left eigenvector u_{ki} determines the share of involvement of an individual modal variable z_i for the corresponding state variable x_k

The eigenvalues are referred to as the modal response and describe the characteristic behavior of the system dynamics. The eigenvalues are in general complex and are expressed as:

$$\lambda = \sigma + j\omega \tag{2.18}$$

with the corresponding frequency of oscillation given by.:

$$f = \frac{w}{2\pi} \tag{2.19}$$

the damping ratio which determines the rate of decay of the amplitude of the oscillation is given by:

$$\zeta = \frac{-\sigma}{\sqrt{\sigma^2 + \omega^2}} \tag{2.20}$$

In the general complex form of eigenvalue given in equation 2.18, the real part represents the damping and the imaginary part represent the frequency of oscillation. Any mode with $w = 0$ represent a non-oscillatory mode. A negative real value corresponds to a decaying mode, a positive damped mode and hence a stable mode. While a positive real

value corresponds to negative damped mode, which represents aperiodic instability[2]. Further details can be found in [2].

2.6.2 Natural Excitation Technique - Eigensystem Realization Algorithm

The Natural Excitation Technique - Eigensystem Realization Algorithm also referred to as NExT-ERA is a twofold method because it consists of two algorithms. The NExT algorithm estimates the impulse responses of the system using cross-correlation functions from the measurement data. The ERA estimates a state-space model based on the impulse responses which are then used to determine the system dynamics. Thereon the modal components can be calculated from eigenvalues of the dynamic matrix of the state-space model.

The method is a three-step process. The first step is to acquire the ambient data of power system variables, such as voltage magnitude, voltage angle, power flow or generator speed.

The second step is to perform the NExT method. First, the auto-correlation of a signal or the cross-correlation between multiple signals is calculated, whereas one of them is a reference. The reference signal corresponds to a variable in the equation of motion for the system, and consequently, therefore, is seen as free responses. The reference variable could, for example, be rotor angular displacement or the air gap power.

The third step is to use ERA to estimate the modal parameters by using the estimated free responses. After the state-space model is estimated, the modal components can be determined.

Natural Excitaiton Technique (NExT)

Consider the swing equation presented in 2.6 and repeated here for convenience.

$$M\frac{d^2\delta}{dt^2} = P_m - P_e - D\frac{d\delta}{dt} = P_{acc} \tag{2.21}$$

Modeling the generator with constant flux linkage, and linearizing the swing equation

2.21 around an operating point, gives

$$M\frac{d^2\Delta\delta}{dt^2} + D\frac{d\Delta\delta}{dt} + K\Delta\delta = 0 \tag{2.22}$$

Where K is the synchronizing coefficient, and $\Delta\delta$ is the rotor angle deviation from the operating point. Considering a power system consisting of n generators, all generators can be represented in the classical form of equation 2.22. Consequently, equation 2.22 become a matrix equation with M, D and K transforming into diagonal matrices containing inertia, damping and synchronizing coefficient of each generator in the system. An elaboration of this modeling can be found in [2].

Furthermore, each generator is consistently exposed to stochastic accelerating power due to random load variations. This excitation is considered the natural excitation of a power system together with minor switching, production change and faults. With the natural excitation taken into consideration, equation 2.22 is extended to

$$\mathbf{M}\Delta\ddot{\boldsymbol{\delta}}(t) + \mathbf{D}\Delta\dot{\boldsymbol{\delta}}(t) + \mathbf{K}\Delta\boldsymbol{\delta}(t) = \mathbf{F}(t) \tag{2.23}$$

where the $(\cdot)$ indicates the derivative with respect to time and $\mathbf{F}(t)$ is the excitation vector. Post multiplying equation 2.23 with a reference displacement angle $\Delta\delta_r(s)$, and taking the expected value on each side yields:

$$\mathbf{M}E[\Delta\ddot{\boldsymbol{\delta}}(t)\Delta\delta_r(s)] + \mathbf{D}E[\Delta\dot{\boldsymbol{\delta}}(t)\Delta\delta_r(s)] + \mathbf{K}E[\Delta\boldsymbol{\delta}(t)\Delta\delta_r(s)] = E[\mathbf{F}(t)\Delta\delta_r(s)] \tag{2.24}$$

Where E[$\cdot$] stand for expected value. Further on, 2.24 can be expressed in terms of correlation functions where $\mathbf{R}(\cdot$ denotes a vector of correlation functions

$$\mathbf{M}\mathbf{R}_{\Delta\ddot{\boldsymbol{\delta}}\Delta\delta_r}(t,s) + \mathbf{D}\mathbf{R}_{\Delta\dot{\boldsymbol{\delta}}\Delta\delta_r}(t,s) + \mathbf{K}\mathbf{R}_{\Delta\boldsymbol{\delta}\Delta\delta_r}(t,s) = \mathbf{R}_{\boldsymbol{F}\Delta\delta_r}(t,s) \tag{2.25}$$

Assuming that $A(t)$ and $B(s)$ are stationary process in $R_{AB}(t,s)$, it can be shown that

for stationary process that

$$R_{A^m B}(\tau) = R^m_{AB}(\tau) \tag{2.26}$$

where $\tau = t - s$ and A^m is the mth derivative of the random process A(t) with respect to time and R^m_{AB} give the mth derivative of the correlation function $R_{AB}(\tau)$ with respect to τ.

The reference rotor displacement angles is assumed weakly stationary process and uncorrelated with future disturbances(future values of $\mathbf{F}(t)$. Which corresponds to $R_{\mathbf{F}\Delta\delta_r}(t, s) = 0$ being true for $\tau > 0$. Thus, 2.25 can be written as

$$\mathbf{M}\ddot{\mathbf{R}}_{\Delta\boldsymbol{\delta}\Delta\delta_r}(t, s) + \mathbf{D}\dot{\mathbf{R}}_{\Delta\boldsymbol{\delta}}\Delta\delta_r(t, s) + \mathbf{K}\mathbf{R}_{\Delta\boldsymbol{\delta}\Delta\delta_r}(t, s) = 0 \qquad \tau > 0 \tag{2.27}$$

Thus, the correlation functions of the rotor angle displacement satisfy the homogeneous equation of motion for the power system in 2.23 which allows the correlation functions obtained to be treated as a free impulse response of the power system. An extended derivation of the correlation functions can be found in [13],[14] and [15]. Since the rotor angle of the generators has a coupling to the other variables such as power flow, voltages and voltage angles, the impulse responses can also be estimated from the correlation functions of these variables. This allows the correlation functions obtained from different PMU data to be used to estimate the total dynamic behavior of the power system.

The NExT can also be used on unsynchronized data. Since it is not treated further in the thesis, it is not explained here. However, theoretical background of it can be found in [4],[5].

Eigensystem Realization Algorithm

The Eigensystem Realization Algorithm is developed by Juang and Pappa [16], and it was made with the goal of finding the minimum realization of the state-space representation of a system by measured responses from a physical system. Realization in control system theory is the matrices $\mathbf{A}, \mathbf{B}$ and $\mathbf{C}$ that form the state-space representation of

the system. Following [16] notation, given a system in the form of

$$\begin{aligned} \mathbf{x}(k+1) &= \mathbf{A}\mathbf{x}(k) + \mathbf{B}\mathbf{u}(k) \\ \mathbf{y}(k) &= \mathbf{C}\mathbf{x}(k) \end{aligned} \tag{2.28}$$

where $\mathbf{A}, \mathbf{B}$ and $\mathbf{C}$ are discrete-time state-space matrices. And $\mathbf{x}(k)$ is the vector of states, $\mathbf{y}(k)$ is a vector of system outputs and $\mathbf{u}(k)$ is a vector of system inputs at the kth step. The ERA can be conducted by first forming Hankel matrix $\mathbf{H}(0)$ and $\mathbf{H}(1)$. A Hankel matrix has the following form [16],[7]

$$\mathbf{H}(k) = \begin{bmatrix} y(k) & y(k+l) & y(k+2) & \cdots & y(k+s-1) \\ y(k+1) & y(k+2) & y(k+3) & \cdots & y(k+s) \\ \vdots & \vdots & \vdots & \vdots & \\ y(k+r-1) & y(k+r) & & \cdots & y(k+r+s-2) \end{bmatrix} \tag{2.29}$$

where $\mathbf{y}(k)$ is the vector of measurements of the system at time k. After running the measurements with NExT, $\mathbf{y}(k)$ becomes the correlation functions and can thus be used with ERA. The parameters r and s corresponds to the number of rows and columns in the Hankel matrix. The values of s and r has to be selected prior to building the matrix, which can be difficult. However, the values of s and r has to be chosen such that the rank of $\mathbf{H}(0)$ does not increase by increasing r ans s. [16] recommend s to be 10 times the number of expected poles and r double of s.

$\mathbf{H}(0)$ can also be written as

$$\mathbf{H}(k) = \mathbf{P}\mathbf{A}^{\mathbf{k}}\mathbf{Q} \tag{2.30}$$

where $\mathbf{P}$ corresponds to the observability matrix and $\mathbf{Q}$ the controllability matrix of the system and looks like

$$\mathbf{P} = \begin{bmatrix} C \\ CA \\ \vdots \\ CA^{r-1} \end{bmatrix} \quad , \quad \mathbf{Q} = \begin{bmatrix} B & AB & A^2B & \cdots & A^{s-1}B \end{bmatrix} \tag{2.31}$$

The $\mathbf{P}$ and $\mathbf{Q}$ matrices has the properties of a rank which equals the minimum model order n for the system. Applying Sylvester's rank inequality [17] theorem, it can be shown that

$$rank(\mathbf{P}) + rank(\mathbf{Q}) - n \leq rank(\mathbf{PQ}) \leq min[rank(\mathbf{P}), rank(\mathbf{Q})] \tag{2.32}$$

$$n + n - n \leq rank(\mathbf{H}(0)) \leq min[n, n] \tag{2.33}$$

$$rank(\mathbf{H}(0)) \leq n \tag{2.34}$$

Which shows that the minimum order of any realization of the system equals the rank of $\mathbf{H}(0)$. However, due to non-linearities and noise, the rank of $rank(\mathbf{H}(0)$ can be significantly higher than the minimum order of the system. Therefore, to estimate the order of the system, singular value decomposition(SVD) is performed on $\mathbf{H}(0)$. The decomposition is of $\mathbf{H}(k)$ is given by

$$\mathbf{H}(k) = \mathbf{U}\mathbf{\Sigma}\mathbf{V}^{\mathbf{T}} \tag{2.35}$$

Where $\mathbf{\Sigma}$ is the diagonal matrix of the singular values of $\mathbf{H}(0)$, $\mathbf{U}$ is a left vector of singular values and $\mathbf{V}$ is the right singular vectors, respectively. The order is estimated by examining the singular values along the diagonal of$rank(\mathbf{\Sigma})$. Singular values that are very small compared to highest singular value correspond to noise, and their columns and rows are omitted from $\mathbf{U}, \mathbf{\Sigma},$, and $\mathbf{V}^{\mathbf{T}}$ matrices. The ratio of each singular value to largest singular value is compared to a threshold which is given by

$$\frac{\sigma_i}{\sigma_{max}} = 10^{-m} \tag{2.36}$$

Where m is an integer that is chosen by the user. In this study, the threshold is set to $10^{-}3$, and any singular values below that threshold are omitted along with their corresponding rows and columns from $\mathbf{U}, \mathbf{\Sigma}$ and $\mathbf{V^T}$. This result in truncated matrices.

The last step in ERA is to obtain the state-space matrices using the truncated $\mathbf{U}, \mathbf{\Sigma}$, and $\mathbf{V^T}$. The discrete-time state-space matrices are calculated by

$$\hat{\mathbf{A}} = \mathbf{\Sigma}^{-\frac{1}{2}}\mathbf{U^T}\mathbf{H}(1)\mathbf{V}\mathbf{\Sigma}^{\frac{-1}{2}} \tag{2.37}$$

$$\hat{\mathbf{B}} = \mathbf{\Sigma}^{-\frac{1}{2}}\mathbf{V^T}\begin{bmatrix}\mathbf{I}_s & \mathbf{0}\end{bmatrix}^T \tag{2.38}$$

$$\hat{\mathbf{C}} = \begin{bmatrix}\mathbf{I}_r & \mathbf{0}\end{bmatrix}\mathbf{U^T}\mathbf{\Sigma}^{-\frac{1}{2}} \tag{2.39}$$

After the discrete-time state-space matrices have been calculated, the modal components can be derived from the state matrix $\hat{\mathbf{A}}$. The eigenvalue from ith mode is given by

$$\lambda_i = \sigma_i + j\omega_i \tag{2.40}$$

with the corresponding frequency and damping of oscillation given by.:

$$f_i = \frac{\omega_i}{2\pi} \qquad\qquad \zeta_i = \frac{-\sigma_i}{\sqrt{\sigma_i^2 + \omega_i^2}} \tag{2.41}$$

Challenges with NExT-ERA

A successful performance of NExT depends on the capability of the systems input parameters to excite all the modes. However, the input parameters are unknown. Besides, the performance relies also on the window length of the measurements observed. The cross-spectral density functions are estimated by "windowing" the data and averaging them in the frequency domain. Thus, having longer records provide more samples to be averaged, and thus a more accurate estimation. The drawback with NExT is that the correlation functions need one reference parameter for the entire set of data records. The reference variable should be a signal located close to where the mode of interest is observable. In power system, the reference PMU records should have high observability of the inter-area modes. If not, there are chances of not detecting the mode or obtaining an answer that deviates from true value is highly increased.

In ERA, the challenges of performing it successful relate to selecting the dimensions to the Hankel matrices and the truncation of the singular values. Choosing too small dimensions makes it difficult for ERA to detect all relevant modes, but the dimension should be large enough such that an increase of dimension does not affect the rank of the Hankel matrix. [16] recommend the columns to be ten times the expected poles, and the rows of the matrix to be double that of the columns. There is, however, another conventional method to select dimensions, according to [4],[16] the Hankel matrix is built making full use of the decaying signal provided the SNR to be high. However, this method depends on the quality of the free responses.

Concerning the singular values, the truncation of singular values has an essential impact on the accuracy of the results. Underestimation leads to modes being omitted from the results, and overestimation leads to inclusion of noise and non-linearities, which consequently can estimate non-existent modes and computational modes. However, it is preferable to overestimate the singular value matrices, since there exist mathematical tools that can differentiate the true modes from fictitious modes generated by noise. It is also easy to which modes that are fictitious, as they have either too high damping or unexpectedly low damping.

2.6.3 Summary of NExT - ERA

The steps in NExT-ERA can be summarized by the following points:

1. Preprocess the PMU measurements to appropiate signals by filtering, detrending and downsampling
2. Select reference parameter to make the correlation functions
3. Calculate the correlation functions
4. Select r(rows) and s(columns) forthe the Hankel matrix
5. Build Hankel matrices $\mathbf{H}(0)$ and $\mathbf{H}(1)$
6. Perform singular value decomposition on $\mathbf{H}(0)$ and truncate the resulting matrices by a ratio determined by $\frac{\sigma_i}{\sigma_{max}} = 10^{-m}$. The rank of the truncated matrices is the order of the system.
7. Calculate state-space matrices $\mathbf{A}, \mathbf{B}$ and $\mathbf{C}$
8. Obtain the eigenvalues from $\mathbf{A}$ and determine the frequency and damping ratio of each mode.

2.6.4 Modal estimation with Multivariate Auto-Regressive Model

Multivariate Auto-Regressive Model(MAR) is as the name implies, a method that can fit multiple time series into Auto-Regressive models(AR) which correlates. The MAR model is also referred to as Vector Auto-Regressive Model and has the same properties as a univariate Auto-Regressive model. Both AR model and MAR model obtain present value from all variables as a linear sum of their past values. The MAR differ from the univariate in that it can take into account the relation between multiple time-series and fit it to vectors of AR models. Such process gives more accurate information on the modal variables related to power systems, as more PMU measurements from different location yields more observability. It should be noted that univariate AR models can also treat multiple signals, but the method does not take into account the relation between the signals, and thus it may not always give the best observability.

Theoretical Background

According to [18] and [19], a MAR model can be decomposed such that eigenvalues are obtained. Obtaining the eigenvalues give the user information on the dynamic behavior of a system. The modal information can be estimated with MAR by decomposition of its coefficient matrices. Given the following AR model of arbitrary order p

$$y_t = \omega + A_1 y_{t-1} + A_2 y_{t-2} + \dots A_p y_{t-p} + \epsilon_t, \tag{2.42}$$

where y_t is a *nx1* random vector, A is a *nxn* matrix and correspond to the coefficient matrix. The ω is *nx1* vector of intercept terms, while ϵ_t correspond to noise and has the same dimension as the intercept terms vector. The MAR(p) model has the same properties as an AR(p) model. Investigating the following AR(1) model

$$y_t = \omega + A_1 y_{t-1} + \epsilon_t, \tag{2.43}$$

for a specific period of t elements, it can be shown that

$$\begin{aligned} y_1 &= \omega + A_1 y_0 + \epsilon_1 \\ y_2 &= \omega + A_1 y_1 + A_2 + \epsilon_2 \\ &= \omega + A_1(\omega A_1 y_0 + \epsilon_1) + \epsilon_2 \\ &= (I_k + A_1)\omega + A_1^2 y_0 + A_1 \epsilon_1 + \epsilon_2 \\ &\vdots \\ y_t &= (I_k + A_1 + \dots + A_1^{t-1})\omega \ + A_1^t y_0 \sum_{i=0}^{t-1} A_1^i + \epsilon_{t-i} \end{aligned} \tag{2.44}$$

This shows that the vectors $y_1, y_2..., y_t$ is determined by its past values and the noise and coefficient matrices. The unknown parameters ω and coefficient matrices can be estimated by a least squares function [19],[18],[4] and other functions as well, such as Yule-Walker least square algorithm [20][4]. The AR (1) can be extended to a MAR model with arbitrary order p because any AR(p) can be written as MAR(p) model.

If y_t is a MAR of order p like in 2.43, there exist a corresponding MAR(1) with $n*p$ dimensional model

$$\begin{bmatrix} y_t \\ y_{t-1} \\ y_{t-2} \\ \vdots \\ y_{t-p+1} \end{bmatrix} = \begin{bmatrix} \omega \\ 0 \\ 0 \\ \vdots \\ 0 \end{bmatrix} + \begin{bmatrix} A_1 & A_2 & \cdots & A_{p-1} & A_p \\ I & 0 & \cdots & 0 & 0 \\ 0 & I & \dots & 0 & 0 \\ 0 & 0 & \ddots & 0 & 0 \\ 0 & 0 & \cdots & I & 0 \end{bmatrix} \begin{bmatrix} y_{t-1} \\ y_{t-2} \\ y_{t-3} \\ \vdots \\ y_{t-p} \end{bmatrix} + \begin{bmatrix} \epsilon_t \\ 0 \\ 0 \\ \vdots \\ 0 \end{bmatrix} \tag{2.45}$$

in a more compact form :

$$\mathbf{y_t} = \omega + \sum_{\mathbf{k=1}}^{\mathbf{np}} \mathbf{A y_{t-1}^k} + \epsilon_t \tag{2.46}$$

Decomposing the coefficient matrices to

$$A = L\Lambda L^{-1}$$

$$A = L \begin{bmatrix} u_1 & 0 & 0 & 0 \\ 0 & u_2 & 0 & 0 \\ 0 & 0 & \ddots & \vdots \\ 0 & 0 & \cdots & u_k \end{bmatrix} L^{-1} \tag{2.47}$$

$$\tag{2.48}$$

Where $\Lambda = \begin{bmatrix} L_1 L_2 \dots L_k \end{bmatrix}$ is a matrix containing columns of eigenvectors which corresponds to the basis of vector space to the state variables y_t. The eigenvalues of the coefficient matrix can be obtained by:

$$\lambda_k = \frac{ln(u_k)}{\tau_s} \tag{2.49}$$

$$\lambda_k = \alpha_k + \omega_k \tag{2.50}$$

Where τ_s is the sampling time of the time series. The damping ratio of the corresponding

mode is found by:

$$\zeta_k = \frac{-\sigma}{\sqrt{\alpha_k^2 + \omega_k^2}} \tag{2.51}$$

Model order selection

One of the main challenges with MAR is the model order selection. The accuracy of the MAR is clearly affected by the order selection [4],[18],[20]. In [18], different algorithms for model order selection based on several different criteria are presented. In [6], the least squares using Schwarz Bayesian Criterion (SBC) [1] for model order selection is used. The author in [6] suggest in [4] the model order for MAR in the range 20 and 24 is suitable for 10 Hz sampling frequency.

Chapter 3

Validation of Identification Methods with Synthetic Signal

To validate the methods implemented in MATLAB, they are tested with a synthetic signal. This chapter shows the results of the estimation by NExT-ERA and MAR for a synthetic signal with and without noise. When there is only a single signal, the NExT estimate the impulse response of the system by auto-correlation of a single signal, and MAR estimate the signal to fit as an AR model.

The signal created for the validation is 3.1 and is presented in figure 3.1.

$$y(t) = 4cos(2\pi 2.5t)e^{0.05t} + 5.5cos(2\pi 5t + \frac{\pi}{8})e^{2.0t} + 2cos(2\pi 0.8t)e^{0.667t} \tag{3.1}$$

Following the Nyquist criteria, the sampling rate is chosen to be 6 times the highest frequency for MAR, NExT-ERA, which result in a sampling frequency of $f_s = 30i$ Hz. The signal is sampled over 10 seconds and is tested with and without noise. There are 3 poles in the synthetic signal, and thus the model order is chosen to be 6 MAR. For NExT-ERA, the columns of the Hankel matrices c becomes $c = 30 * 6$, which makes the rows r 180. The order of the NExT-ERA is chosen to be the number corresponding to all the singular values larger that are larger than $0.1 * \sigma_{max}$ in ERA, which is 6.

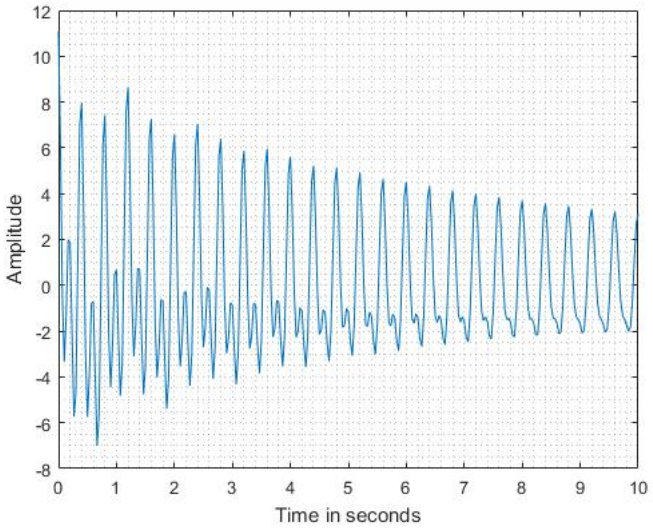

Figure 3.1: Synthetic signal without noise

3.1 Noise Free Signal

Table 3.2 shows the resulting estimation of NExT-ERA, MAR and a comparison with the robust prony algorithm. Table 3.1 shows the corresponding eigenvalues. As it can be seen from table 3.2, the methods is capable of estimating the modes of interest in the synthetic signal for a model order of 6. These results are not post-filtered. However, MAR was not as accurate for the initial model order of 6 and were tried for different model orders.

Table 3.1: Estimated eigenvalues of the synthetic signal without noise

Eigenvalues [rad/s]	
NExT-ERA	**MAR**
-0.2000 +31.4159i	*-0.2001 +31.4159i*
-0.2000 -31.4159i	*-0.2001 -31.4159i*
-0.0500 +15.7080i	*-0.0503 +15.7083i*
-0.0500 -15.7080i	*-0.0503 -15.7083i*
-0.6670 + 5.0265i	*-0.6170 + 4.9804i*
-0.6670 - 5.0265i	*-0.6170 - 4.9804i*

Table 3.2: Estimated results of the synthetic signal without noise

NExT-ERA				MAR			
frequency [1/s]	Damping ratio	Phase [rad]	Amplitude	frequency [1/s]	Damping ratio	Phase [rad]	Amplitude
5.0001	0.0064	-0.3927	5.5000	5.010	0.00636	-0.3927	5.5008
2.5000	0.0032	-0.0000	4.0000	2.5001	0.0032	0.0015	4.0044
0.8070	0.1315	0.0000	2.0000	0.7987	0.1230	-0.0486	1.9297

Using least squares with Schwarz's Bayesian Criterion (SBC) for model order estimation , which are used in [18] and [21], suggest that the model order for the signal should be 37 for MAR. But, it does not have to be that large as, a lower order estimate the signal perfectly and makes the computation faster. The model order were tested for 8,10,16,20 and 37. The lowest model order with accurate result were 8, which are presented in table 3.3.

Table 3.3: Estimated result with MAR when the model order is 8

MAR			
frequency [1/s]	Damping ratio	Phase [rad]	Amp
5.0001	0.0064	0.3927	5.5000
2.5000	0.0032	0.0000	4.0000
0.0107	1.0000	3.1416	0.0413
0.8070	0.1316	-0.0007	2.0001

3.2 Signal with Noise

The synthetic signal is added white Gaussian noise with a SNR of 5. Before running the algorithms, the signal is filtered with a second order high-pass and low-pass filter with a cut off frequency of 0.5 Hz and 6 Hz respectively. Then a spectral analysis is conducted to see if the desired frequency components are visible. It can be seen from figure 3.2 that the filtering is able to make the 0.8 Hz mode visible, which otherwise is not visible with the added noise.

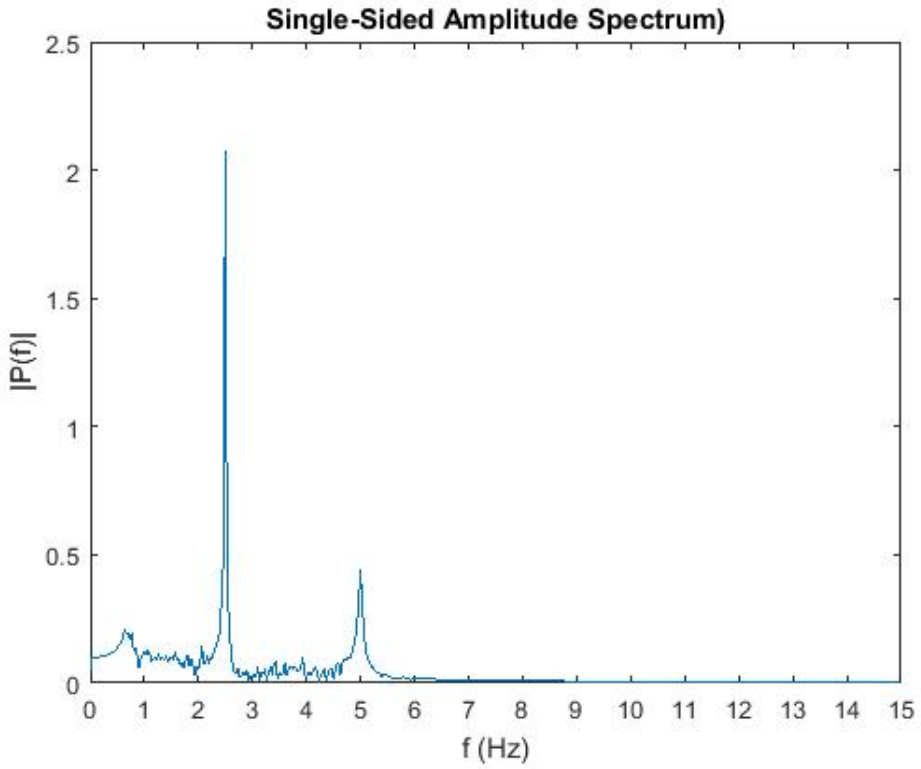

Figure 3.2: Spectrum of filtered the synthetic signal with noise

Prior to conducting the identification, the model order is to be selected. In ERA, the order is chosen to be 6. This is based on the computed singular values in figure 3.3that are larger than $0.1 * \sigma_{max}$, suggested by [22], while for MAR model order is chosen to be 55, approximated by least squares using Schwarz's Bayesian Criterion (SBC) for model order estimation.

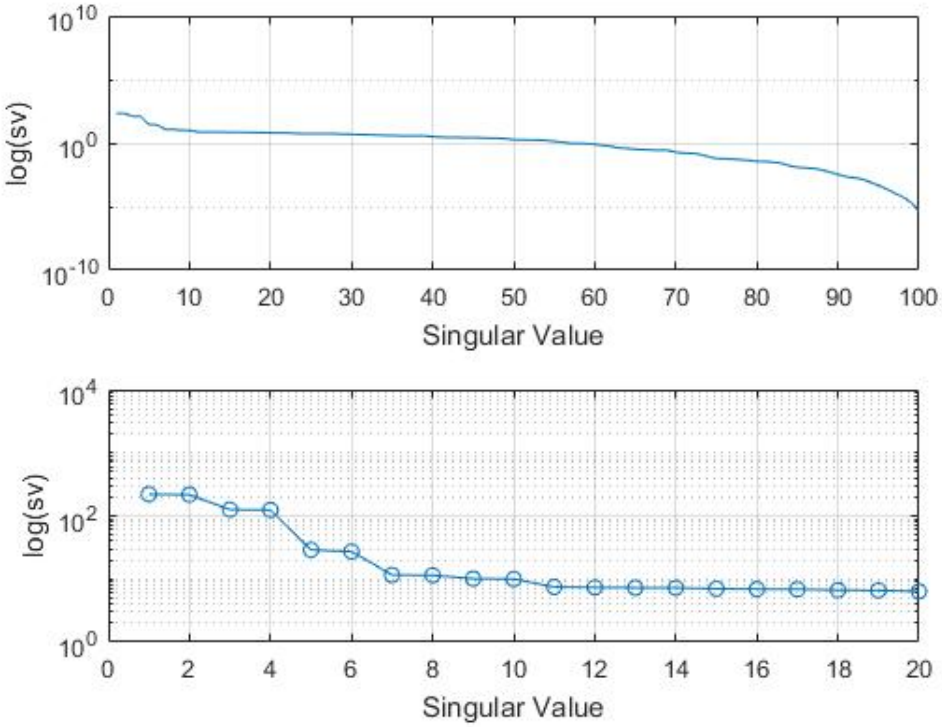

Figure 3.3: Singular Values of the noised signal

The sampling rate is the same and the window length is 10 seconds. Conducting the identification, it can be seen from table 3.4 that ERA and MAR is capable of estimating frequency and damping components of the noised signal, but struggles to approximate the damping of the 0.8 Hz. With added noise, MAR generates components which is not present in the original signal without noise. This is a result of not being able to choose the right model order best fitted for the signal. An inaccurate model order computes fictitious components. Thus, the model order were reduced to 20, which gave accurate estimation with a less computational modes.

Table 3.4: Estimated result of the synthetic signal with noise

NExT - ERA			MAR		
Frequency	**Damping**	**Damping ratio**	**Frequency**	**Damping**	**Damping ratio**
4.9971	-0.2011	0.0064	11.8798	-1.3524	0.0181
2.5004	-0.0571	0.0036	10.2628	-2.1088	0.0327
0.8201	-0.6701	0.0833	8.8215	-2.7748	0.0501
			7.8514	-1.4216	0.0288
			6.4732	-1.1543	0.0284
			5.0006	-0.1924	0.0061
			2.4993	-0.0636	0.0041
			0.8094	-0.7307	0.1437

The same analysis is conducted for a longer window length. The length of the signal is now increased to 1 minute seconds with a sampling frequency of 30 Hz. And the window length is increased by 10s for each estimation up to 1 minute. Figure 3.4 and 3.5 show the performance of ERA and MAR as the window is increased. Only the desired modes is plotted. MAR generated computational noise, while ERA did not.

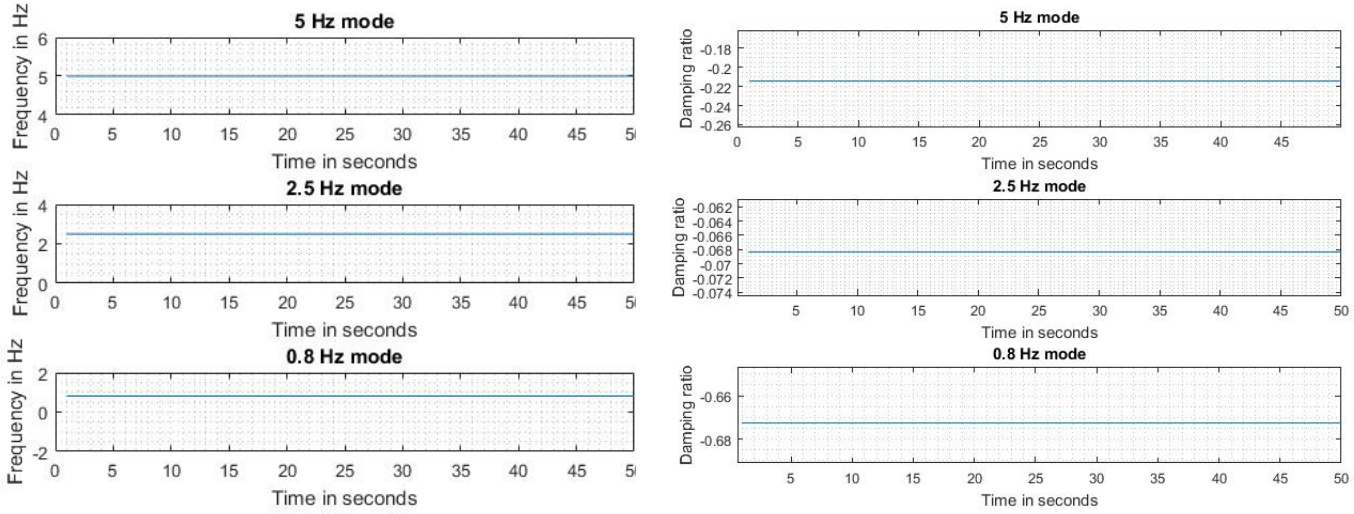

(a) Frequency estimate by ERA **(b)** Damping estimate by ERA

Figure 3.4: Mode estimate of lowest damped inter-area modes by ERA.

As it can be seen from figure 3.4, both frequency and damping estimation by ERA is consistent even though the window length is increased.

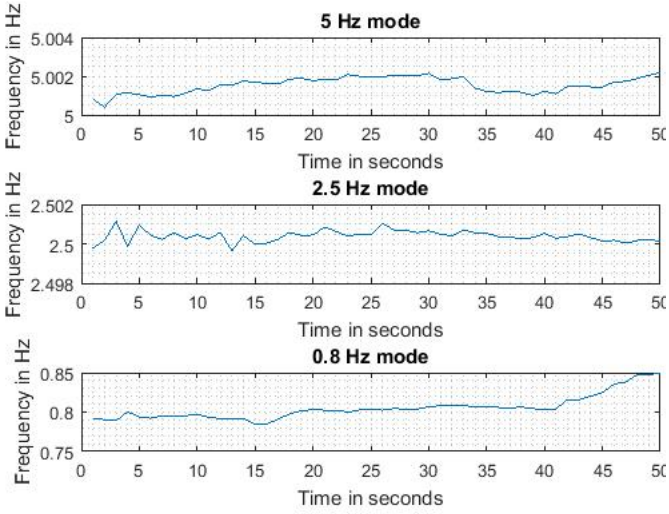

(a) Frequency estimate by MAR

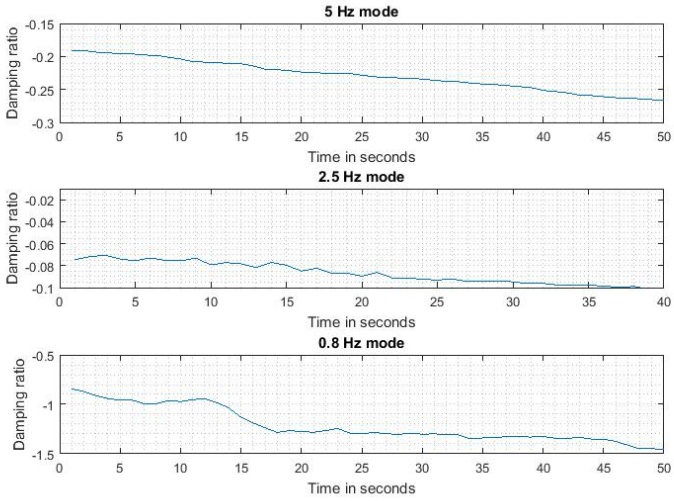

(b) Damping estimate by MAR

Figure 3.5: Mode estimate of low damped inter-area modes by MAR

MARs estimation of the frequency resulted very accurately,but the estimation of damping deviates from the actual value as the window size increases.

Chapter 4

Linear Analysis of Nordic Test Grid

In this chapter, the performance of the method is examined by comparing inter-area modes estimated NExT-ERA and MAR with obtained modes from linearized power system model in PowerFactory.

4.1 Simulation Software - DigSILENT PowerFactory

DigSILENT's PowerFactory is a power system software with the capability to model the behavior of a power system, from synchronous machines to transformers and transmission lines, and down to load. It is effectively used to study faults, power flow, state estimation, stability analysis and more.

In this project, PowerFactory is chosen, to use simulated data of a test network, as a mean to validate the system identification methods. This is conducted by carrying out a modal analysis with PowerFactory inbuilt linear analysis function to estimate the modal response of the inter-area modes with poor damping. These estimations are later used to validate the system identification modes.

To validate the system identification methods, signals from simulated data in the test network are used as measurements. To emulate PMU data from PowerFactory, each load is perturbed with Gaussian white noise for different signal to noise ratio(SNR) to obtain a model with ambient responses. Then, a selected number of nodes are used as measurement point based on the nodes observability, and measurement data are extracted.

4.2 Nordic 44 Test Model

The Nordic 44 model is a test network developed at NTNU customized for analysis of power system phenomena that can also be analyzed analytically. The test network represents the Norwegian, Swedish and Finnish grid. The Norwegian grid consists of 8 areas denoted as NO 1 to NO 8 and is connected to the Swedish grid through two-lines between Hasle and Ringhals and Jarpend and Hagaasen. While the Norwegian grid is connected to the Finnish in Varangerbotn in the north. The Swedish grid is divided into four areas, denoted as SE1 to SE4, and connects to the Finnish grid through Porjus and Grundforsen. The Finnish grid has two areas. The single line diagram of the test network is shown in the figure below. The network consists of 44 buses, hence its name. In the original version, it consists of 45 loads, 23 active generators and 3 active wind turbines in each area. The Nordic 44 has also included NorNed and NordLink which is the tie-line connection between North Netherlands and Germany from Norway respectively, the Nordbalt link between Sweden and Lithuania and the Estlink connection between Finland and Estland.

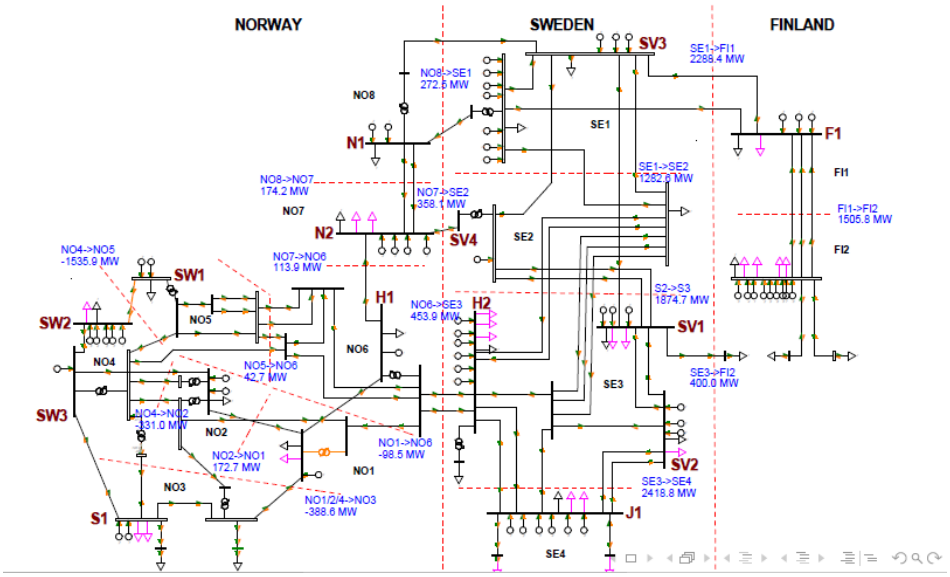

Figure 4.1: Line diagram of Nordic 44 test system

The network has gone through many iterations of updates from the original network, more of the changes can be found in [23]. The latest version of the Nordic 44 for PowerFactory was tailored for a study on stability analysis of future scenarios of the Nordic Power Systems by Lester Kalemba, in that version the total load and generation were half of what current load and generation of the Nordic power system is, and thus

the inter-area modes were non-existent. To excite the inter-area modes and obtain a test network that reflects the current power system the load and generation were increased a substantial amount by using data from an equivalent Nordic 44 model from PSSE. The details of changes and alterations can be found in appendix .1.

A summary of N44 components is shown in table 4.1 and its loading in table 4.2.

Table 4.1: N44 Components summary

No. Of Substations	*3*	*No. Of Busbars*	*50*	*No. Of Terminals*	*36*	*No. Of Lines*	*70*
No. Of 2-W Trfs	*16*	*No. Of 3-W Trfs*	*0*	*No. Of Syn.Machines*	*44*	*No. Of Asyn.Machines*	*0*
No. Of Loads	*44*	*No. Of Shunts/Filters*	*0*	*No. Of SVS*	*0*		

Table 4.2: Load flow Summary

	MWA	*MVA*	*MVAr*
Generation	*52484,19*	*11268,69*	*53680,29*
External Infeed	*0*	*0*	*0*
Load P(U)	*52235,05*	*13081*	*53848,05*
Grid Losses	*249,14*	*-1812,31*	
Line Charging	*0*	*-5828,44*	
Installed Capacity	*1314833,3*		
Spinning Reserve	*15285,76*		

4.3 Modal Analysis of Nordic 44

Before perturbing each load with Gaussian white noise, a small signal stability analysis is conducted in PowerFactory on Nordic 44 to estimate the lowest damping of the inter-area modes. The small signal stability analysis resulted in 405 modes, whereas the lowest damping modes of inter-area modes were mode $f_1 = 0.666$ Hz and $f_2 = 0.927$ Hz. Their modal components are shown in table 4.3. The 0.66 Hz mode is poorly damped, while 0.927 Hz mode is slightly above the 5% boundary for what is considered poorly damped [3].

Table 4.3: Result of modal analysis in PowerFactory. The table shows the lowest damped inter-area modes.

Frequency	*Eigenvalue[1/s + rad/s]*	*Damping ratio*
0,666	*-0,1373 + j4,1854*	*0,0328*
0,666	*-0,1373 - j4,1854*	*0,0328*
0,927	*-0,4389 + j5,8225*	*0,0752*
0,927	*-0,4389 - j5,8225*	*0,0752*

The corresponding mode shapes for the modes in 4.3 are shown in figure 4.2. The plots show the state variable of generator speed and only the 15 first synchronous machines which are most observable. Both plot legends show the generator speed in descending order of magnitude in mode shape.

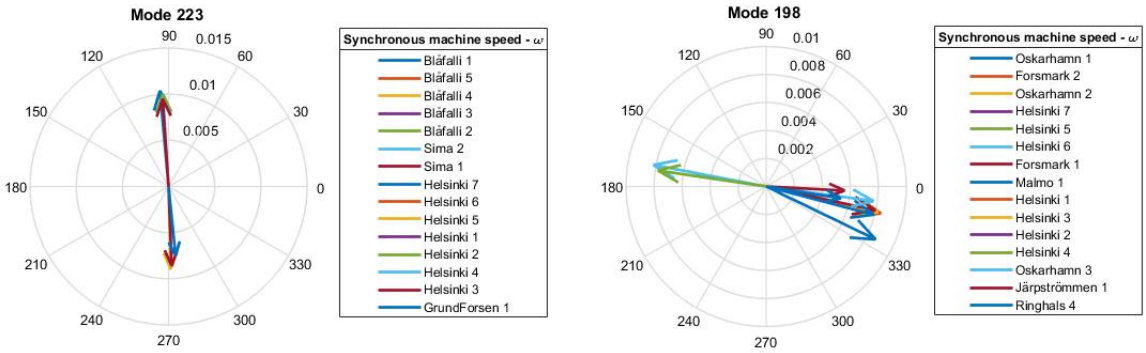

(a) $f_1 = 0.666$ Hz Mode **(b)** $f_2 = 0.927$ Hz Mode

Figure 4.2: Modeshapes of lowest damped inter-area modes. The plot is of speed state.

When exposed to 0.666 Hz mode it is clear that the most observable generators are at Blåfalli together with generators in Sima. These generators are the one's vector arrows pointing upwards in 4.2a at almost 90 degrees, whereas Blåfalli generator 1 is the one with the most significant magnitude. These generators are swinging against the generators at Helsinki and the generator at Grundforsen which points in opposite direction of the generators at Blåfalli and Sima. Thus, it can be said the southern and western part of Norway is swinging against Finland and eastern part of Sweden. These swings are greatly involved in forming the inter-area oscillation at mode 223.

The 0.927 Hz mode with damped frequency of 0.9267 Hz has the generators at Helsinki swinging against generators in Sweden, the generators in Oskarshamn, Forsmark, Malmo, Jarpstrømmen and Ringhals. The generators in Finland are the ones pointing to left with approximately 180 degrees, and the Swedish generators pointing to the right. The most observable generator in Sweden is Oskarshamn generator 1, while in Finland is Helsinki generator 7.

4.4 Analysis of Simulated Data from Nordic 44

To emulate PMU measurements, each load in Nordic 44 is perturbed with SNR of 5, 10 and 25. Each identification method is tested for all signals containing all three SNRs, to test how robust they are. A SNR of 5 corresponds to the poorest measurement a PMU have. PMU has typically a higher SNR than 5, ranging between 5 and 30[6].

4.4.1 PMU Placement in Nordic 44

The modes obtained in section 4.3 in table 4.3 are used as comparison for the simulated data. The most observable components are in South-West Norway, South Sweden and Helsinki in Finland. Simulated data are extracted from Blåfalli, Kristiansand, Trondheim, Ringhals, Oskarshamn, Grundforsen and Helsinki. The placement is based on the observability in the network based on the modal information on the most observable generators, the nodes with the majority connections to other nodes and inter-area transmission. The measurement taken on these nodes are active power from one of the generators and voltage angle, whereas Blåfalli is used as a reference.

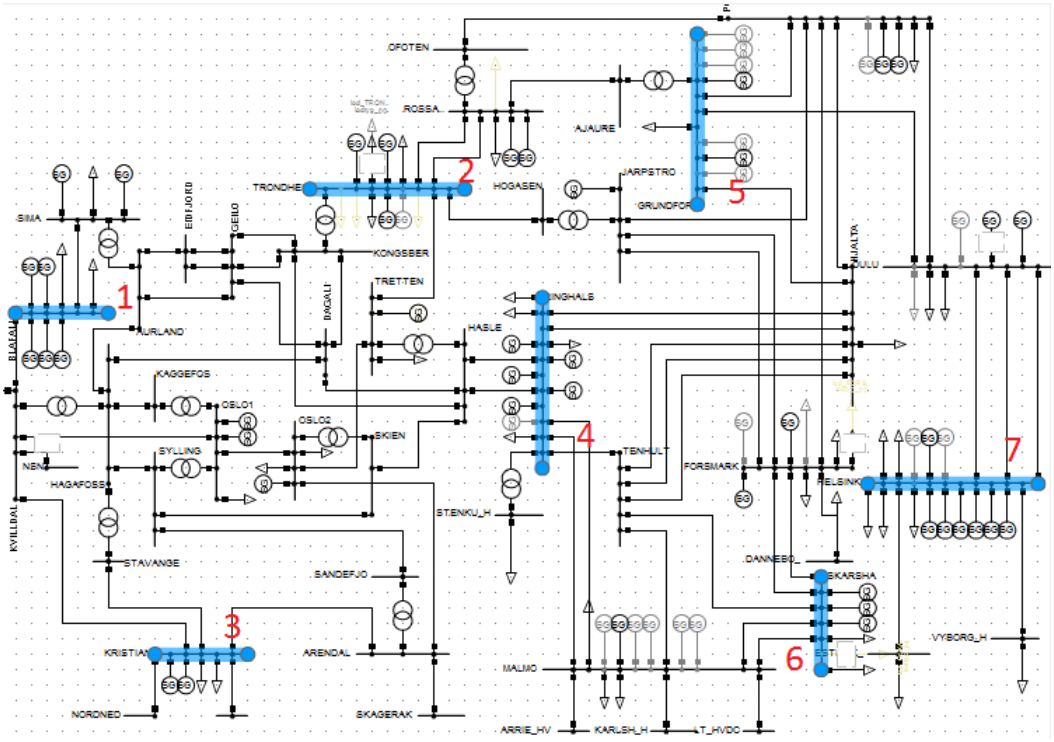

Figure 4.3: PMU Placement in Nordic 44. The blue colored nodes correspond to nodes with PMU

The placements are shown in figure 4.3 and the numbering in red correspond to Blåfalli, Trondheim, Kristiansand, Ringhals, Grundforsen, Oskarshamn and Helsinki in that order.

4.4.2 Simulated data

The data extracted for testing were simulated for a SNR of 5, 10 and 25. The data simulated is 20 minutes with a sampling frequency of 10 Hz. The same data is filtered by a high-pass and low-pass filter with a cut-off frequency at 0.1 Hz and 2 Hz. The means are removed from the signal before estimation.

Before the estimation, a spectral analysis is conducted to identify the dominant frequency in the signal. It can be seen in 4.4 for the active power measurements that the $f_1 = 0.666$ Hz and $f_1 = 0.927$ is present in the signal. Also, another frequency component which is dominant, but not of interest.

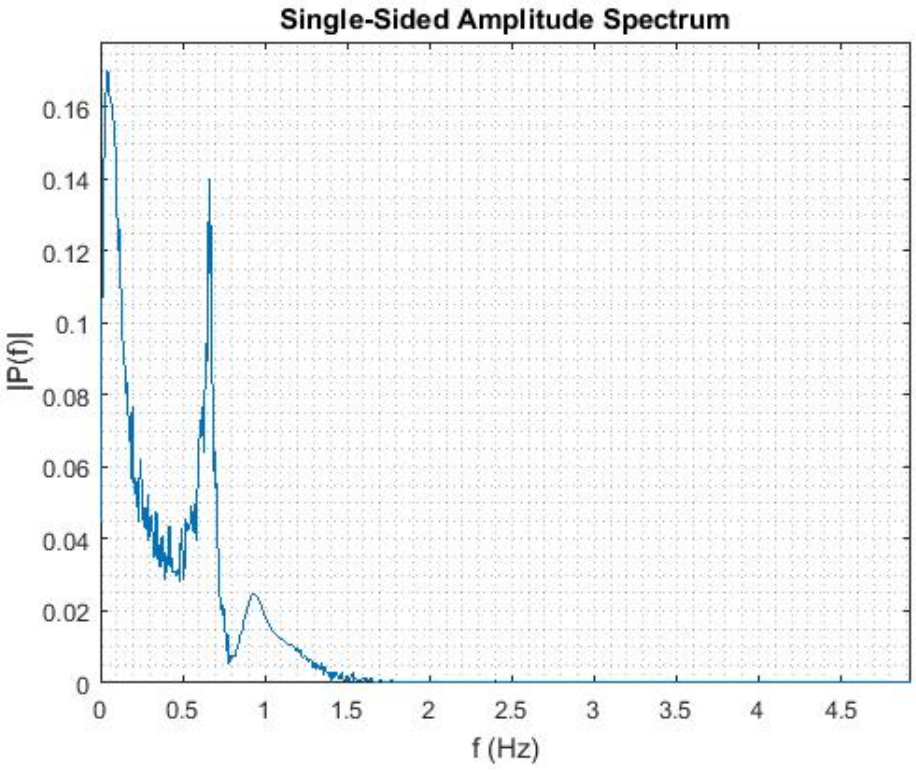

Figure 4.4: Spectral density of simulated active power data

The optimal order of MAR is calculated to be 66 using least squares with Schwarz's Bayesian Criterion (SBC). The model order for NExT-ERA is chosen automatically based on the singular values truncation method. The columns of the Hankel matrices c is chosen to be $c = 30 * 10$, which makes the rows r 600. The window length of the measurements is increased 1 minute, for all measurements taken.

4.4.3 Ambient analysis

Results for SNR = 5

The initial estimation of active power for a window length of 20 minutes is shown in table 4.4, and for voltage angle in 4.5. The active power as the signal results in the 0.666 Hz mode being rather accurate for the frequency and damping ratio by both algorithms. While the 0.927 Hz mode estimation by both algorithms is acceptable for the frequency but inaccurate for the damping ratio. The frequency estimation of the 0,927 Hz is acceptable since its deviation is approximately 5%.

Table 4.4: Modal estimation with active power as signal

NExT-ERA		MAR	
Frequency	**Damping ratio**	**Frequency**	**Damping ratio**
0.9409	0.0846	0.9895	0.1255
0.6655	0.0336	0.6579	0.0328

The estimation using voltage angle measurements as a signal resulted in 4.5. The table indicates that the methods are capable of estimating using voltage angle as a signal. However, the estimation is somewhat inaccurate. The frequency estimation of the 0.666 Hz mode is rather accurate for both algorithms. The damping ratio deviates for both MAR and NExT-ERA by 18%. The frequency estimation of the 0.927 Hz mode by NExT-ERA deviates by 2% and is rather accurate for damping ratio. While the estimated frequency of MAR has a 4% deviation, and damping ratio has 9% deviation, which is close.

Table 4.5: Modal estimation with voltage anlge as signal

NExT-ERA		MAR	
Frequency	**Damping ratio**	**Frequency**	**Damping ratio**
0.9537	0.0720	0.9675	0.0684
0.6641	0.0388	0.6506	0.0269

The modal estimation is conducted for a window length up to 20 minutes, with updates each minute. Figure 4.6 shows the result with voltage angle as signal and figure 4.5 show the result with active power as the signal. As it can be seen, the estimation is rather constant for both algorithm apart from MARs damping estimation of 0.667 Hz

mode. This show that the noise has little effect on the identification if the length is sufficient enough.

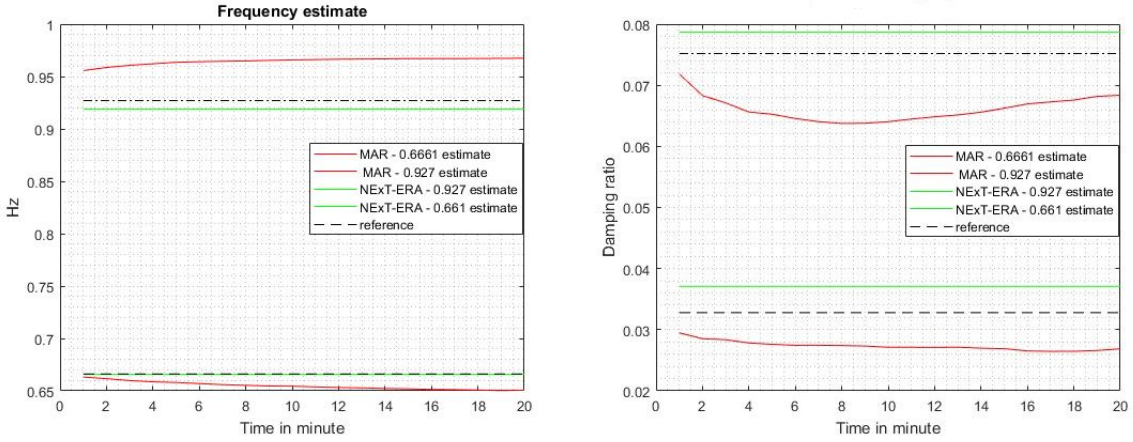

(a) Frequency estimated **(b)** Damping estimated

Figure 4.5: Modal estimation based on active power measurements for a SNR = 5

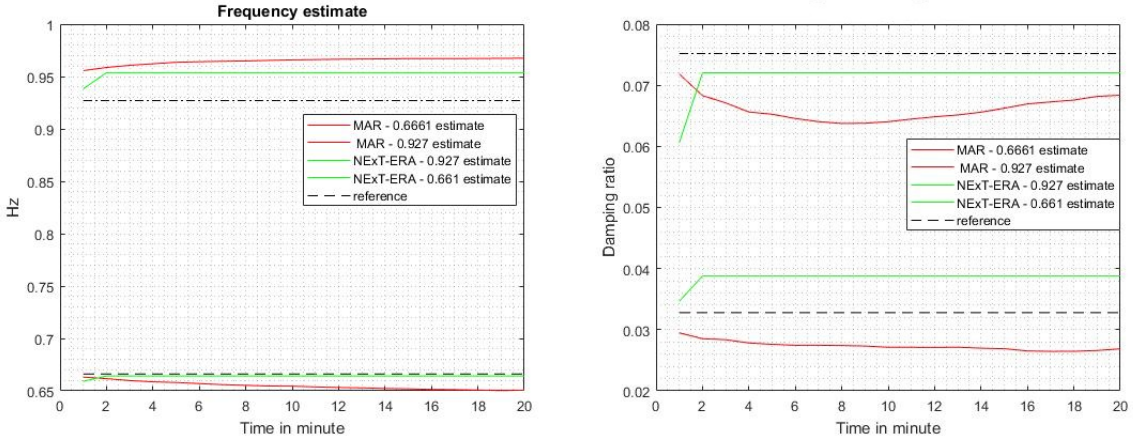

(a) Frequency estimated **(b)** Damping estimated

Figure 4.6: Modal estimation based on voltage angle measurements for a SNR = 5

Results for SNR = 10

For SNR of 10, the noise is less, and thus it is expected a better estimation. Figure 4.7 and 4.8 shows the damping and frequency estimation when the signal has a $SNR = 10$. The NExT-ERA estimated satisfactory results of the frequency and the corresponding damping components when using active power as the input signal. While the MAR has

a good estimation of the 0.6661 Hz mode but struggles to estimate the 0.927 Hz mode accurately. The deviation is 13% at worst for the frequency and 112% for damping ratio estimate when the window length is 20 minutes.

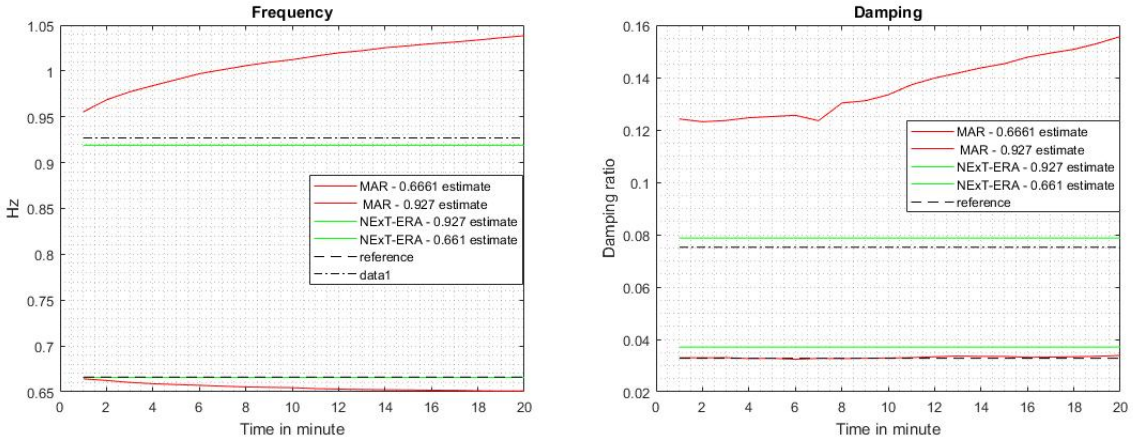

(a) Frequency estimated **(b)** Damping estimated

Figure 4.7: Modal estimation based on active power measurements for a SNR = 10

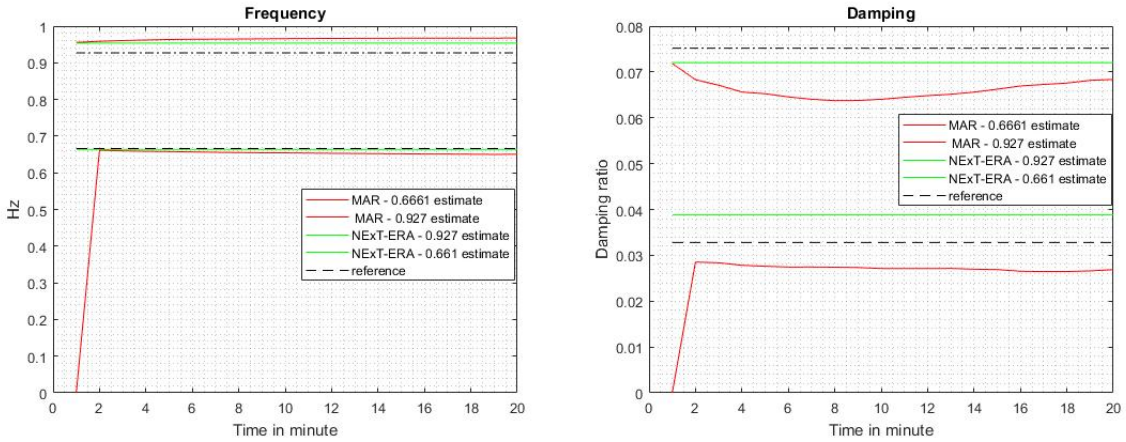

(a) Frequency estimated **(b)** Damping estimated

Figure 4.8: Modal estimation based on voltage angle measurements for a SNR = 10

Using voltage angle as the signal, the MAR estimation of frequency component becomes highly more accurate for 0.927 Hz mode. The 0.6661 Hz mode estimated is also accurate, but its corresponding damping ratio estimate deviates more than 10%. While the damping ratio for 0.927 Hz mode deviates with 5% at best and 12,23% at worst. The same is true for the estimation by NExT-ERA. The frequency estimated is highly

accurate, but their corresponding estimated damping ratio deviates by 14% and 5% for the 0.6661 Hz mode and 0.927 Hz mode respectively.

Results for SNR = 25

With a SNR of 25, the estimates of frequencies of interest are rather accurate estimated for both methods when the active power signal is used as a signal. For the of 0.666 Hz mode, the damping ratio is rather accurate. Both methods have an estimate of damping ratio which deviate less than 3% from the actual damping ratio. The damping ratio estimation 0.927 Hz mode is farther away from the actual damping, the NExT-ERA estimate a damping ratio of 0.078, while MAR estimates a damping ratio of 0.082. Which makes a deviation of 3,7% and 9% respectively.

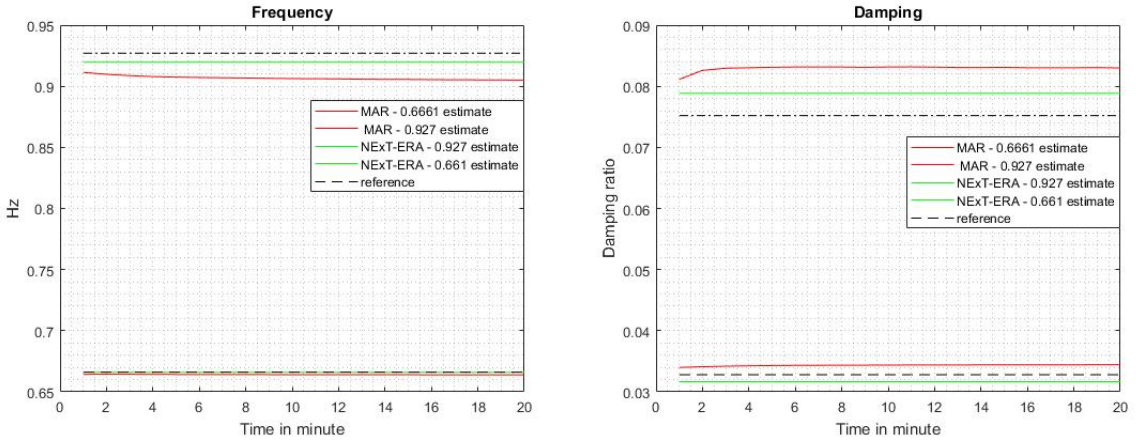

(a) Frequency estimated **(b)** Damping estimated

Figure 4.9: Modal estimation based on active power measurements for a SNR = 25

The same accuracy on estimation of the frequency is obtained with voltage angle as measurement, apart from NExT-ERA estimation on 0.927 Hz mode. The NExT-ERA estimation on 0.927 Hz mode is 0.95 Hz and deviates by 2% which is satisfactory. The damping ratio estimates is rather accurate for the estimation on 0.666 Hz mode damping ratio, but deviates for the 0.927 Hz mode. The estimated damping ratio by NExT-ERA on 0.927 Hz mode is 0.08 which deviates by 6,4%, while MAR best estimation is 0.085 and deviates as the window length extends. At worst, MAR estimates the damping ratio of 0.927 Hz mode to be 0.09 which is approximately 20% off the 0.0752

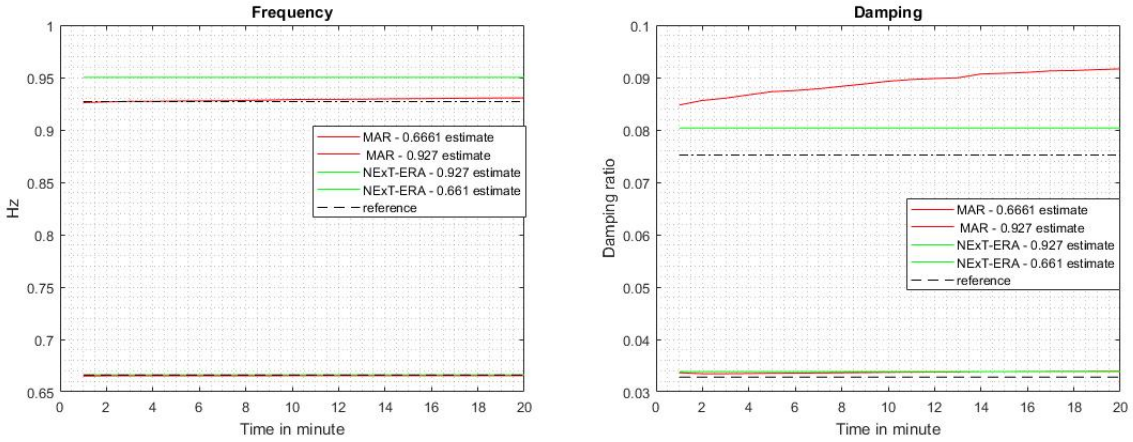

(a) Frequency estimated **(b)** Damping estimated

Figure 4.10: Modal estimation based on voltage angle measurements for a SNR = 25

Chapter 5

Linear Analysis of PMU data

In this chapter, an analysis of the modal identification methods presented in this thesis is going to be conducted based on its performance with real PMU data. The PMU data and its associated mode are presented, together with the process of pre-processing the data. Further on a spectral density analysis is conducted to verify the mode of interest before a thorough analysis is conducted. The analysis is based on the window length, the model order and the size of the Hankel matrix.

5.1 Analysis of PMU data

In this section, real PMU data are used to test the performance of the methods. The data is provided by Statnett through Kjetil Uhlen and Dinh Thuc Duong. The extracted PMU data are measurements of active power on the transmission lines connected to Varangerbotn in the Nordic power system grid and the power flow between Hasle and Halden. Varangerbotn lies in northern Norway where it is close to northern Finland borders. The transmission lines measured are the connection between Varangerbotn, Adamselv, Ivalo(Finland) and Kirkenes. The connection between Varangerbotn and Ivalo is a dominant inter-area path and based on experience and studies, where there has been observed 1 Hz mode with an approximately 5% damping.

Hasle lies in the south-east of Norway and is close to the Swedish border and connects the Norwegian grid with the Swedish. The Hasle-Halden connection is Norwegian, and this will be used to identify the inter-area oscillation known to be seen in Halden. In this area, a 0.5 Hz mode has been observed by Statnett[Uhlen], with damping approximately 10%. The damping varies and can be 2-3% deviation in Varangerbotn and 3-4 % deviation in Hasle. All these are approximated since the conditions of a power system

changes all the time, and thus it is difficult to assure which values that are entirely correct. These modes also listed in table 5.1 is the modes of interest in this chapter. They which will be used as a benchmark for the performance for MAR and NExT-ERA.

Table 5.1: Modes observed in Varangerbotn and Hasle.

	Varangerbotn	***Hasle***
Frequency	*∼1.0 Hz*	*∼0.5 Hz*
Damping ratio	*∼5%*	*∼10%*

5.1.1 Data pre-processing

Figure 5.1 shows the measurements extracted.The flow of the power is from Kirkenes to Varangerbotn and Varangerbotn towards Ivalo and Adamselv. While in Hasle, the power flow from Hasle to Halden. The measurement is taken for 1 hour with a sampling frequency of 10 Hz.

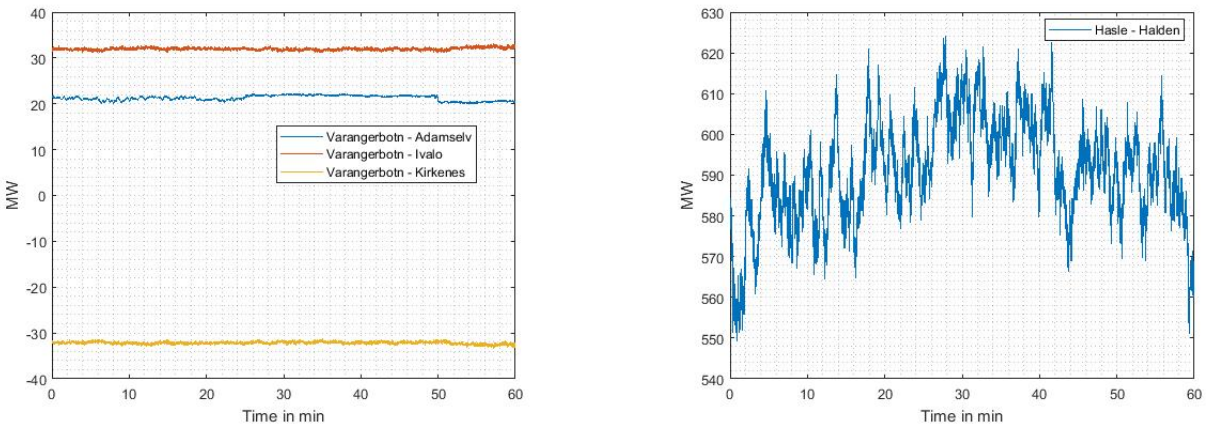

(a) Measurement in Varangerbotn **(b)** Measurement in Hasle

Figure 5.1: PMU measurement of active powerflow in Hasle and Varangerbotn

Prior to analyzing the signals, the data is filtered with a Butterworth high-pass and low-pass filter with $f_{c1} = 0.1$ Hz and $f_{c1} = 2$ Hz respectively. The high-pass filter is used to remove unwanted low frequency components, while the low-pass filter is used to remove high frequency noise. The choice of cut-off frequency corresponds to the range in which electromechanical modes can be found, such that essential information is not lost.

5.1.2 Spectral Analysis of PMU Data

Before the identification is conducted, a spectral analysis is performed to identify the prominent frequencies in measurement data. This is done to verify that the modes of interest are there. Figure 5.2 and 5.3 shows the spectral density functions of Varangerbotn and Halden, respectively. The method used to plot spectral density function is Welch's power spectral density function in MATLAB.

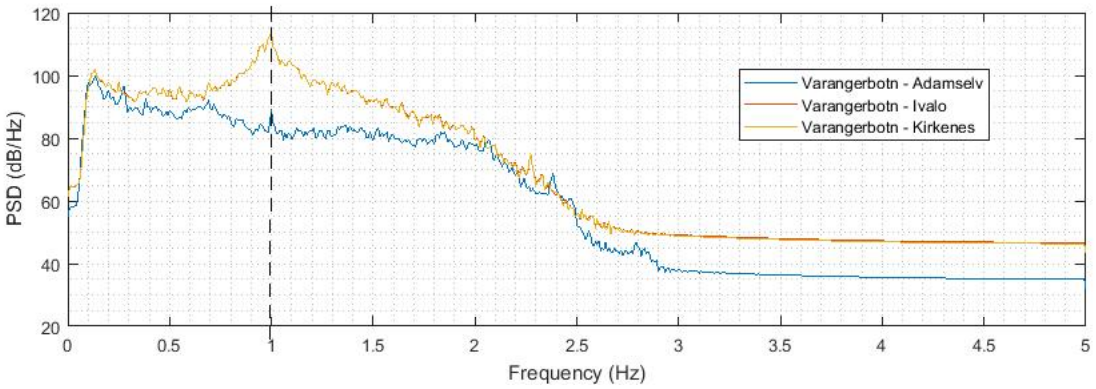

Figure 5.2: Spectral density function of active power in Varangerbotn

From figure 5.2, all measurements from each connection spectral density is plotted. The Varangerbotn - Ivalo spectral estimate lies upon the Varangerbotn - Adamselv estimate. The dashed line is a reference to the observed mode in Varangerbotn from table 5.1. As shown in the figure, the mode of interest is one of two primary component. The other primary component is 0.14 Hz. Observe also that the 0.1 Hz frequency component is not significant in Varangerbotn - Kirkenes spectral estimate, and thus it may not be as easy to detect in that connection compared to the other two.

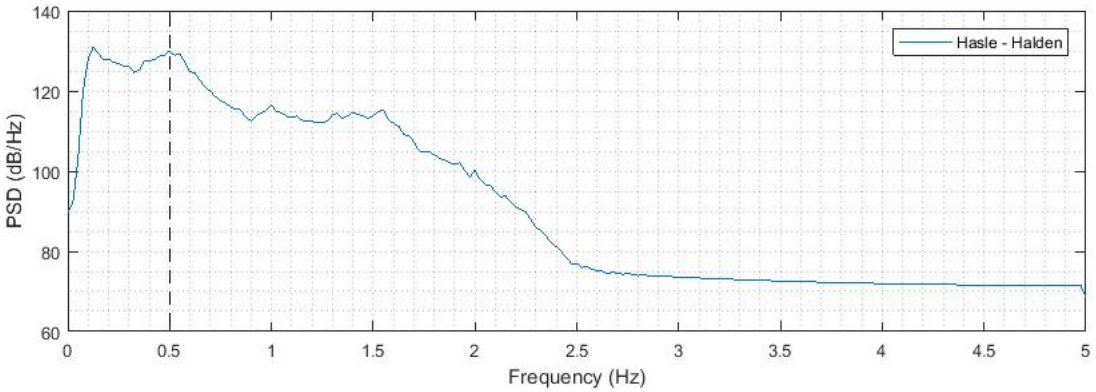

Figure 5.3: Spectral density function of active power in Hasle

In Hasle there also two prominent components. From figure 5.3 there is a 0.5 Hz component which is the mode of interest. In addition, the 0.14 Hz component and 1 Hz component can also be observed.

By conducting a spectral analysis on the measurements on, the modes of interest is verified to be among the PMU data extracted.

5.1.3 Modal analysis of PMU data

In this section, the performance of NExT-ERA and MAR based on Hankel matrix size, model order selection and window length are presented. The analysis is presented in two-part. First, the MAR is being tested for different model order and window length. Then NExT-ERA performance is presented for different Hankel matrix size and window length. The estimation by both algorithms is performed on the data obtained from Hasle and Varangerbotn separately and also in conjunction. This is to evaluate if the dominant modes in one place can be seen in another.

First, the modal identification is conducted in Varangerbotn, then in Hasle, and last when the measurements are in conjunction. The model order was chosen to be 20 based on [6] and the findings in specialization project. The size of Hankel matrix in ERA is chosen to be 120x240. This is based on that there are 3 dominant modes in the spectral density analysis, and accordingly, to [24],[5],[22], which states the columns should be 20 times the frequencies and rows double of columns. The size was doubled as the initial results did not estimate the desired frequency. The reference for NExT is chosen to be Varangerbotn - Ivalo measurements since the mode of interest has the highest observability there. The window size was chosen to b 60 minutes with a sampling frequency of 10 Hz. The time elapsed time were 0.646290 seconds for both algorithms running simultaneously.

Estimated mode with measurements from Varangerbotn

Table 5.2 show the resulting modes estimated by both algorithms from measurements in Varangerbotn. The NExT-ERA is capable of estimating the dominant frequencies observed in the spectral analysis and their corresponding damping ratio. The first mode estimated by NExT-ERA coincide well with the 1.0 Hz mode that is known to oscillate in Varangerbotn. This deems the estimation as a success and capable. However, the estimation is not capable of locating 0.5 Hz mode that is known to oscillate in Hasle.

The size of the Hankel matrix was expanded to evaluate if the dynamics were not included, but only computational modes were generated.

Table 5.2: Estimated modes with measurements from Varangerbotn.

	NExT-ERA		MAR	
No	Frequency[Hz]	Damping ratio [%]	Frequency[Hz]	Damping ratio [%]
1	0.9942	5.5686	1.8251	1.4938
2	0.1025	11.5226	1.8359	1.5553
3			1.7155	2.2287
4			1.2183	6.1550
5			0.9951	3.4823
6			1.0535	9.9183
7			0.4909	40.0022
8			0.2924	36.0018

Similar to NExT-ERA, the estimation by MAR was not able to identify the 0.5 Hz mode seen in Hasle. The corresponding damping ratio of the estimated 0.5 Hz mode in table 5.2 is too high and thus not representative. This mode is deemed as computational mode, along with mode 8 in table 5.2. The other modes estimated are not known if they are fictitious or real. However, the modes that coincide with 1.0 Hz mode known to be in Varangerbotn is mode 4 and 5, which is a close approximation. However, which of them is the computational mode or not is difficult to tell.

Estimated modes with measurements from Hasle

The same estimation is conducted with measurements in Hasle, and their result is shown in table 5.3. Similar to estimation by data in Varangerbotn, the NExT-ERA is not capable of estimating the 1.0 Hz mode in Varangerbotn using measurements in Hasle. The first mode in table 5.3 coincide with expected estimation of 0.5 Hz mode. If this is, the mode representing the 0.5 Hz is difficult to say, since the second mode is also within the frame of expectation. Comparing the second mode estimated by NExT-ERA and the fourth mode estimated by MAR. It can be concluded that second mode estimated by NExT-ERA and the no fourth mode by MAR is the corresponding estimate of the expected 0.5 Hz mode.

Table 5.3: Estimated modes with measurements from Hasle

	NExT-ERA		MAR	
No	Frequency[Hz]	Damping ratio [%]	Frequency[Hz]	Damping ratio [%]
1	0.5108	12.9317	1.9616	0.8298
2	0.4418	6.1686	1.5902	1.7001
3	0.1136	16.1564	1.1951	4.9782
4	0.2443	15.4069	0.5736	7.1516
5			0.2307	25.6863

The 0.1 Hz mode which is dominant in the signal is also estimated by NExT-ERA, but the damping ratio is however increased which is not coherent with the measurements in Varangerbotn. The fourth mode by NExT-ERA is not of interest as it is well damped and have not any impact on the system. The first, second and fifth mode estimated by MAR are computational modes. The third mode estimated by MAR is coherent with the 1.0 Hz mode known to be in Varangerbotn and may be the same mode.

Estimated modes with measurements from Hasle and Varangerbotn in conjuction

Using data from Varangerbotn and Hasle yield the modes in table 5.4. The estimation of the known 1.0 Hz and 0.5 HZ by both methods is coherent with the findings with estimation using the PMU data separately.

Table 5.4: Estimated modes with measurements from Hasle and Varangerbotn together

	NExT-ERA		MAR	
No	Frequency[Hz]	Damping ratio [%]	Frequency[Hz]	Damping ratio [%]
1	0.9727	6.1192	1.1995	5.0170
2	0.4040	8.9397	1.1448	5.2804
3			0.7152	17.2621
4			0.5728	7.2153

Estimation with different order by MAR

The estimation conducted for different orders with MAR is performed with a fixed window length of 20 minutes. The order is increased by one up to 60. The modes of no

interest are post-filtered out. The resulting estimation for each model order on data of Varangerbotn is shown in figure 5.4. The estimated frequency component is consistent with the increasing model order and the reference mode of 1 Hz. The estimation of damping ratio is however inconsistent with the change of model order. The expected value is 5%, and estimated damping ratios vary around the expected damping ratio which indicates that MAR is functional, but is prone to give biased information if the model order does not fit.

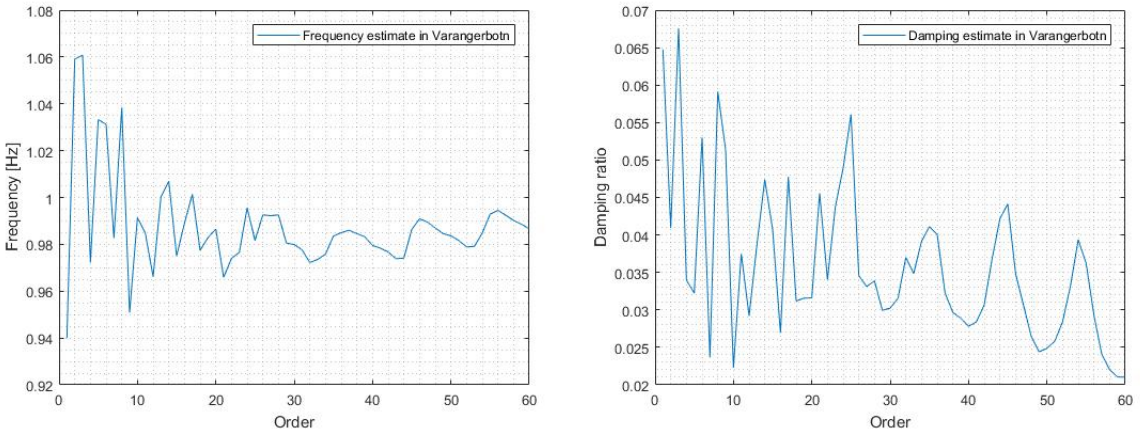

(a) Frequency estimate **(b)** Damping estimate

Figure 5.4: Modal estimation in Varangerbotn for different model orders

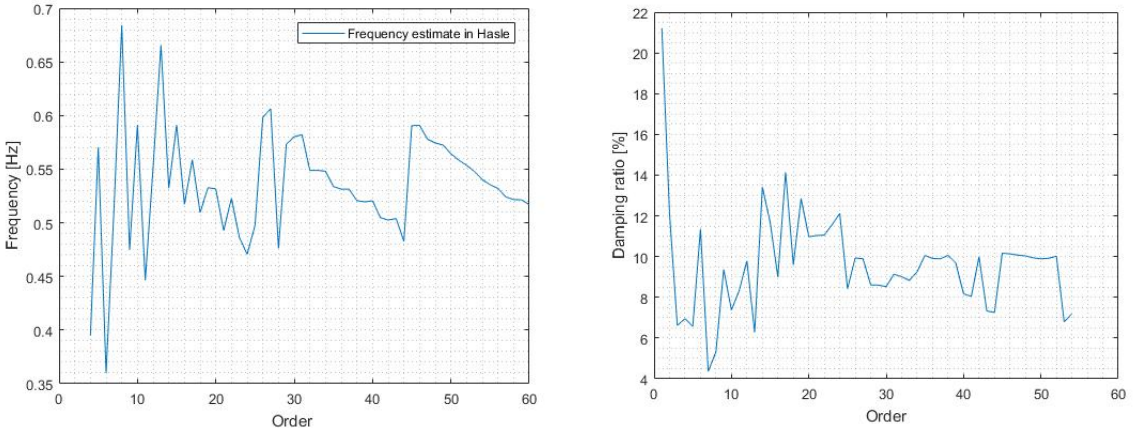

(a) Frequency estimate **(b)** Damping estimate

Figure 5.5: Modal estimation in Haslefor different model orders

Similar observations are made of estimation conducted with data from Hasle. In figure

5.5 it can be seen that the most significant variance is when the model order is low for both frequency and damping estimation. As the model order increases the variations are less and coincide more with the expected mode in Hasle, which is 5% and a damping ratio between 6 10%.

The model order which coincides best with the expected modes is between 20 and 25 which also corresponds with suggested model order [6].

Estimating the modes for different model order with the measurement in Varangerbotn in conjunction with the measurements in Hasle yielded the result in figure 5.6. The orange curve corresponds to the estimation of 0.5 Hz observed in Hasle, and the blue curve corresponds to 1.0 Hz mode in Varangerbotn. The results are coherent with the findings above when the estimation is performed using measurements separately.

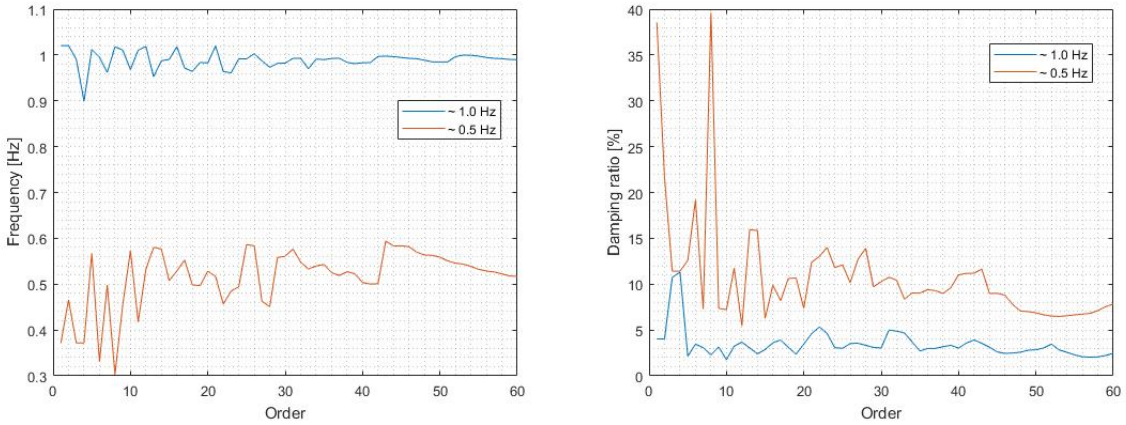

(a) Frequency estimate **(b)** Damping estimate

Figure 5.6: Modal estimation in Varangerbotn for different model orders

Estimation with increasing window by MAR

The estimation with a window increasing is conducted with the model order of 20. The total window size is 60 minutes. Estimations are conducted each minute up to 60 minutes, with the initial window size being 1 minute.

The resulting estimation with measurements from Varangerbotn is shown in figure 5.7 together with estimation with measurements from Hasle. The estimation is done separately. The estimation of the 1.0 Hz mode in Varangerbotn is rather accurate. In the frequency and damping estimate it can be seen that before a window size of 10, the estimation is not consistent with damping estimate. As the window size increase

beyond 10 minutes, the estimation becomes more consistent and coincide well with the expected result and earlier findings in table 5.2 and 5.4. Similar results are obtained with measurements from Hasle.

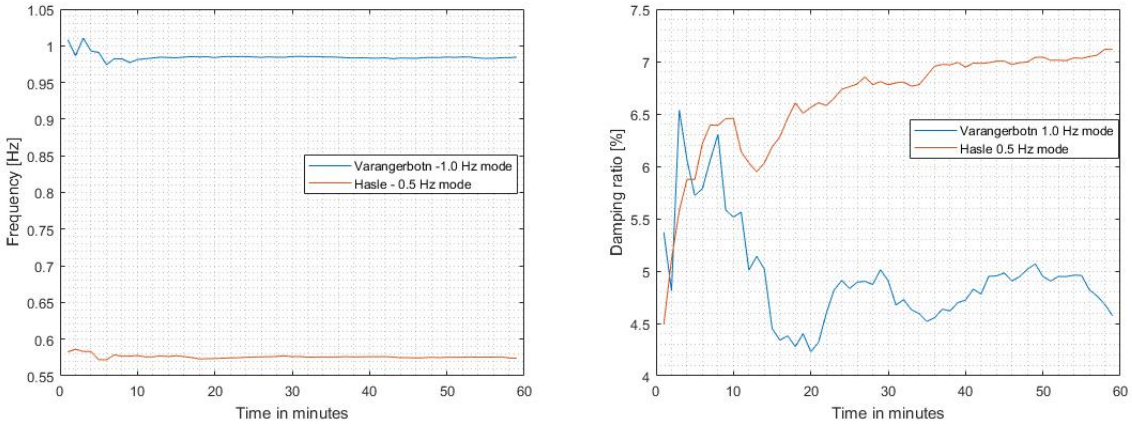

(a) Frequency estimate **(b)** Damping estimate

Figure 5.7: Modal estimation with increasing window size. The estimation shown is done with data individually from each area

The same estimation conducted with measurements in Varangerbotn and Hasle together yielded almost identical results as when the estimation is done separately. Figure 5.8 show the result. The damping ratio estimated in Varangerbotn is more consistent than the one in figure 5.7.

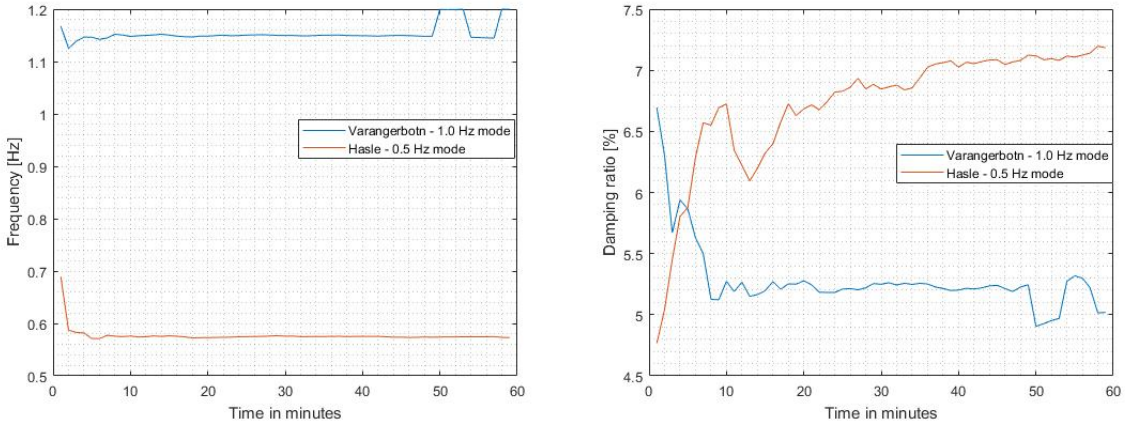

(a) Frequency estimate **(b)** Damping estimate

Figure 5.8: Modal estimation with increasing window size from measurements in Varangerbotn in conjunction with measurements in Hasle

Estimation for different Hankel matrix size with NExT-ERA

Table 5.5, 5.6 and 5.7 show the modal estimation by NExT-ERA for different Hankel matrix size. The same approach of estimating using only measurements from the individual area and subsequently estimating with measurements from both area together is used.

The numbers of rows and columns in the Eigensystem Realization Algorithm are one of the main parts of the algorithm. As the size expands, more elements from the cross-correlation functions are included, and thus more dynamic properties are taken into account. However, oversizing the Hankel matrix may include noise and which subsequently may generate dynamically. The selection of the size becomes iterative if the dynamic properties are not known. In this section, the estimation with NExT-ERA is tested with the size of the matrix ranging from 200x100 to 800x400. The first column show, the input parameter which is multiplied by 10 (expected poles)[5],[16]. The third row shows the elapsed time.

Table 5.5: Estimated modes with measurements from Hasle using NExT-ERA

Varangerbotn				
n	Size [rxp]	Computation Time [s]	Frequency [Hz]	Damping ratio [%]
10	200x100	0.151620	0.9826	5.92
20	400x200	0.656044	0.9815	5.57
30	600x300	1.669735	0.9800	5.08
40	800x400	2.829884	0.9769	4.28

The estimation with data from Varangerbotn shown in table 5.5 show that the algorithm is capable of estimating the 1.0 Hz mode known to be in Varangerbotn. Comparing the results with findings in table 5.2 when n is 6, it can be seen that the estimation is consistent and coherent. As the size increases, the computation time increases.

Table 5.6: Estimated modes with measurements from Varangerbotn using NExT-ERA

Hasle				
n	Size [rxp]	Computation Time [s]	Frequency [Hz]	Damping ratio [%]
10	200x100	0.34	0.5229	11,74
20	400x200	0.496707	0.4932	13.5035
30	600x400	1.259946	0.4867	9.11
40	800x400	2.338633	0.4496	12.16

Similar to findings in Varangerbotn, the findings with data from Hasle in table 5.6 shows that the estimation is consistent with the first mode found in table 5.3, except for the third mode found. This may be due to as the size of the Hankel matrix increases, more elements from the measurements are included, and thus as mentioned in [16], the calculation can become less accurate.

Table 5.7: Estimated modes with measurements from Varangerbotn and Hasle together using NExT-ERA

Varangerbotn + Hasle				
n	Size [rxp]	Computation Time [s]	Frequency [Hz]	Damping ratio [%]
10	200x100	0.196462	0.9711	5.57
			0.3902	7.44
20	400x200	0.708910	0.9700	5.15
			0.3965	3.57
30	600x300	1.690378	0.9706	4.4636
			0.4982	1.1575
40	800x400	3.245818	0.9630	3.4701
			0.4008	1.4026

Table 5.7 show results estimated by the ERA when the measurements are put together.The first estimation when the size is 200x100 is coherent with the findings table 5.4. As the size increases, the results for damping ratio become biased. The damping ratio becomes less and less accurate compared to the result in table 5.4. This can be due to that more elements from the measurements are included in the estimation and thus more dynamic properties

Chapter 6

Summary

6.1 Discussion

The main objective of this thesis is to test the performance of stability indicators based on phasor measurements. Before the method was applied to real PMU measurement, a synthetic signal and simulated data emulating PNU measurements were used to demonstrate the functionality of the algorithm. The results obtained in chapter 3 and 4 prove that the implemented algorithms are functional and capable of estimating the modal component in signal and multiple signals with and without noise. In chapter 5, estimation on real PMU data is presented and proves it is applicable for real-time data. The method shows accurate estimation on the frequency component in all demonstrations, but its estimation on damping ratio varies.

Despite the accuracy of the frequencies estimated by both algorithms, In real-time analysis, and in many cases, the damping ratio estimate is the variable which interests the operators most. However, that is the variable that is often difficult to estimate, since the actual damping ratios of power systems are unknown. As the dynamic changes in the power system, so do the damping ratios. In addition, during ambient operation, the damping ratio may vary significantly as a function of time and the non-linearity. The following sections discuss some of the aspects and findings that influence the estimations

6.1.1 Model order

Specifying the right model order in system identification is one of the essential steps in the estimation. If the model order is to low, some of the dynamic properties may

be excluded in the estimation. This is true for both NExT-ERA and MAR method. Overestimating the model order may generate computational modes by the algorithms. Selecting model order is a difficult task, and there is no exact procedure for it. In this thesis, both MAR and NExT-ERA is tested for different model order.

This thesis starts off by choosing the model order iteratively. The least square method for model order selection for MAR using Schwarz's Bayesian Criterion (SBC) suggested by [18] is used. The initial result by selecting a model order for MAR based on the amount of frequency component yielded an accurate estimate with small insignificant deviation. A more accurate estimation was obtained by increasing the model order slightly. However, this followed a computational mode. And had no significance at that stage. Further on using the suggested model order based on the aforementioned method yielded too high model order, and thus many more fictitious modes. To reduce the number of fictitious modes generated, a model order of 20 were used as a basis. The same approach was used in chapter 4 and gave rather accurate results with less computational modes. In chapter 5, the performance of MAR is tested for different model orders. The presented result using real PMU measurement prove that a model order of 20 and higher give a consistent estimation, and also concludes what other studies have shown.

However, this approach is not efficient, and in an online operation, there is no time to test for different model orders. There exist automated algorithms for model order selection which should be investigated and tried out extensively. The least squares method using Schwarz's Bayesian Criterion (SBC), is such a method and should be further investigated along with Aikake's Finer prediction Error[18].

Similar to MAR, the NExT-ERA modal identification is dependent on choosing the right model order. In NExT-ERA, notably the ERA algorithm, the dimension of the Hankel matrix has to be chosen as well as the model order. The size of the Hankel matrix determines the number of elements from the measurements(cross-correlation functions) that are included further in the estimation. Building a low-rank Hankel matrix may result in missing dynamic information. On the other hand, overestimating the Hankel matrix could lead to computation inaccuracy[16]. This can be seen in chapter 5 where estimation is conducted for different Hankel matrix size. The damping ratio becomes less accurate for estimated damping ratio as the size increases. In addition, the computational time increases which make the method non-applicable for real-time online estimation. The suggested method of choosing the Hankel matrix dimension based on the number of modes in the signal proved accurate, but in real-time such knowledge will not be evident for a system operator. This area should be researched in the same manner as MAR, a method to automatically select the size of the Hankel matrix.

What is great about the NExT-ERA algorithm is two things, the cross-correlation functions and the truncation based on the singular value. The truncation of the singular values matrices based on the number of singular values that are larger $0.1 * \sigma_{max}$ produced for the most part estimation without computational modes. The truncation number also corresponds to the model order and makes it less difficult to analyze the result. However, it should be noted that if the Hankel matrix is forced to be low-rank, the model order (truncation number) may need to be slightly higher to include other dynamic.

6.1.2 Window length and effect of noise

As mentioned in the section above, one of the pros about NExT-ERA is the cross-correlation functions. The cross-correlation functions between two measurements cancel out the noise. This is evident also in the few computational modes estimated by NExT-ERA. It should also be pointed out that the NExT algorithm in the NExT-ERA method, is dependent on having a reference signal for calculation of the cross-correlation functions. The reference signal in this thesis was chosen based on the spectral density analysis conducted in chapter 5, and the most observable generator in chapter 4. It should be further investigated how choosing other reference signal affect the estimation since it is an important point step in estimation.

In this thesis it is found out that the window length for estimation with NExT-ERA is dependent on the Hankel size as explained in the section above, thus increasing the window length has no significance if the Hanke matrix is low-ranked. This is evident in the constant estimation conducted in chapter 3,4 and 5.

However, the analysis window length plays a particular part in estimation with MAR. As seen both in chapter 3 and 4 and 5, the estimation of the frequency component is rather accurate compared to the damping ratio. The estimation of noised simulated data and synthetic signal proved to give an inaccurate estimate of the damping ratio by MAR as the window length were increased. This contradicts with findings in other literature [6],[18] which have done similar studies. The suspicion lies in the added noise with an SNR of 5. Perhaps, the filter used was not good enough. However, the same conclusions are taken in chapter 4 when simulated data is used to imitate PMU measurement. In chapter 5 it is shown that as the window size increases the estimation by MAR becomes more consistent, which is coherent with expected results and other similar studies.

6.1.3 Wide Area Estimation

The applicability for wide area estimation is demonstrated with simulated data and real PMU data. The result presented in chapter 4 and 5 show clear indication that NExT-ERA and MAR are applicable for wide area estimation. In chapter 5, the modal identification is performed iteratively by estimating with measurements from each area individually first, then together. This is conducted to confirm the mode expected to be in each area corresponding to the estimated through modal identification. The problem that presents itself is to know which mode corresponds to which area, for that individual mode. Another problem discussed along the way is to know which mode is real and which is fictitious. In NExT-ERA, it is possible to compute the mode shapes corresponding to an individual mode estimated, however, this is an uninvestigated territory and should be examined how it can be applied to power system-

6.2 Conclusion

This thesis presented two methods of stability indicators that can be used with multiple phasor measurements. The Natural Excitation Technique is used in conjunction with Eigensystem Realization Algorithm. The NExT utilize the cross-correlation between measurements to determine impulse responses of the power system, which can be used in ERA to estimate the state-space model of the power system. Similar, the Multivariate Auto-Regressive model fits the measurement data to multiple AR models which are a linear combination of each other. With multiple signals, the observability of the power system enhances and makes it possible to monitor more of the system dynamics.

The performance of NExT-ERA and MAR was evaluated in three stages. First, a synthetic signal was used to validate the algorithms. Secondly, a test network was used to test the performance with multiple signals by comparing inter-area modes estimated with NExT-ERA and MAR with modes from the linearized test network in PowerFactory. The focus of this chapter was how estimation varied for different size of the window length. Last, real PMU data from the Nordic grid were used to evaluate the performance of the method for different window length and model order.

The results in all three stages indicate that NExT-ERA and MAR are functional and capable of estimating inter-area modes. Both algorithms show that they can estimate for small window length, which is essential for real-time operation. In addition, it was seen that noise had little effect on NExT-ERA, but the MAR had problems when the

window length becomes very large for the simulated data. However, this was not the instance for real PMU data. The estimated results were consistent for long and small window size.

It was also shown that very high Hankel matrix size(model order) for NExT-ERA give an inaccurate estimation. However large Hankel matrix dimension is not desired as the computation time increases to several seconds. Low-rank Hankel matrix proved accurate and sufficient. For MAR, the model order was proved to be consistent when it became 20 or higher. This suggests that a model order of 20 must be used for MAR on real PMU data.

In conclusion, both algorithms presented can detect the modal frequency and the corresponding damping ratio from real PMU measurements, with short and long record length. The result presented in this thesis indicates that NExT-ERA and MAR can be utilized to study the electromechanical modes in power system off-line, and that is possible to implement them for online estimation as well.

6.3 Future Work

The steps for a successful identification follows selecting a data records and their length, pre-processing the data record such that only inter-area modes are visible and the amount of noise is limited, then choosing the model order before estimating. To implement the identification, these steps need to be automated. So far, the only step which proves to be an issue for online estimation is the model order selection. An automatic method to select the model order and in particular for ERA, the Hankel matrix dimension need to be further investigated, to give it online applicability. Another issue, in using multiple signals is that estimated modes do not indicate which area they correspond to. A suggestion could be using multiple signals from a small number of nodes located far from each other, and simultaneously use multiple signals from local measurements connected to the same node and investigate which mode from wide area estimation correspond to local estimated modes. To perform this routine, it is worth mentioning that NExT-ERA is capable of utilizing unsynchronized measurements for estimation. The Natural Excitation Technique introduce a time synchronization error, which is introduced in the correlation functions. More of this can be found in [5].

References

[1] P. K. *et al.*, "Definitions and classification of power system stability", *IEEE Transactions on Power Systems*, vol. 16, no. 2, May 2004.

[2] J. Machowski, J. W. Bialek, and J. R. Bumby, *Power System Dynamics - Stability and Control*, 2nd ed. John Wiley & sons, Ltd., 2008.

[3] P. Kundur, *Power System Stability and Control*. McGraw-Hill, Inc., 1994.

[4] J. M. Seppänen, L. C. Haarla, and J. Turunen, "Modal analysis of power systems with eigendecomposition of multivariate autoregressive models", in *2013 IEEE Grenoble Conference*, Jun. 2013, pp. 1–6. DOI: 10.1109/PTC.2013.6652230.

[5] J. M. Seppänen, J. Turunen, M. Koivisto, N. Kishor, and L. C. Haarla, "Modal analysis of power systems through natural excitation technique", *IEEE Transactions on Power Systems*, vol. 29, no. 4, pp. 1642–1652, Jun. 2014.

[6] J. M. Seppänen, L. C. Haarla, and J. Turunen, "Modal analysis of power systems with eigendecomposition of multivariate autoregressive models", in *2013 IEEE Grenoble Conference*, Jun. 2013, pp. 1–6.

[7] E. B. *et al*, "Identification of electromechanical modes in power systems", Jun. 2012. [Online]. Available: http://sites.ieee.org/pes-resource-center/files/2013/11/TR15_Modal_Ident_TF_Report.pdf.

[8] C. W. Taylor, "The future in on-line security assessment and wide-area stability control", in *2000 IEEE Power Engineering Society Winter Meeting. Conference Proceedings (Cat. No.00CH37077)*, vol. 1, 2000, 78–83 vol.1.

[9] C. Rehtanz, J. Béland, G. Benmouyal, S. Boroczky, C. Candia, D. Cirio, S. Corsi, D. Galvan, R. Grondin, J. Hauer, L. Hornyak, S. Imai, M. Ingram, I. Kamwa, V. Kolluri, P. Korba, M. Larsson, B. Marinescu, Y. Mitani, and M. Zima, "Wide area monitoring and control for transmission capability enhancement", Feb. 2007.

[10] A. R. Messina, Ed., *Inter-Area Oscillations in Power Systems, A Nonlinear and Nonstationary Perspective*. Springer US, 2009.

[11] L. Ljung, *System Identification, Theroy for the User*, 2nd ed., T. Kailath, Ed. Prentice Hall, 2006.

[12] J. G. Proakis and D. K. Manolakis, *Digital Signal Processing (4th Edition)*. Upper Saddle River, NJ, USA: Prentice-Hall, Inc., 2006, ISBN: 0131873741.

[13] G. James, T. Carne, and J. Lauffer, "The natural excitation technique (next) for modal parameter extraction from operating wind turbines", Feb. 1993.

[14] G. James, T. Carne, and J. Laufer, "The natural excitation technique (next) for modal parameter extraction from operating structures", vol. 10, Jan. 1995.

[15] G. James, T. Carne, J. Lauffer, and A. R. Nord, "Modal testing using natural excitation", vol. 2, Jan. 1992.

[16] J. Juang and R. Pappa, "An eigensystem realization algorithm for modal parameter identification and model reduction", vol. 8, Nov. 1985.

[17] B. Kramer, "Model and data reduction for control, identification and compressed sensing", PhD dissertation, Virginia Polytechnic Institute and State University, 2015.

[18] T. Schneider and A. Neumaier, "Algorithm 808: Arfit - a matlab package for the estimation of parameters and eigenmodes of multivariate autoregressive models", Nov. 2000.

[19] H. Lütkepohl, *New Introduction to Multiple Time Series Analysis*. Berlin, Heidelberg: Springers, 2005, ch. Power System Dynamics and Stability.

[20] J.M.Seppänen, J. Turunen, L. C. Haarla, M. Koivisto, and N. Kishor, "Analysis of electromechanical modes using multichannel yule-walker estimation of a multivariate autoregressive model", in *IEEE PES ISGT Europe 2013*, Oct. 2013, pp. 1–5. DOI: 10.1109/ISGTEurope.2013.6695272.

[21] A. Neumaier and T. Schneider, *Algorithm 808: Arfit — a matlab package for the estimation of parameters and eigenmodes of multivariate autoregressive models*.

[22] E. A. Johnson, H. F. Lam, L. S. Katafygiotis, and J. L. Beck, "Phase i iasc-asce structural health monitoring benchmark problem using simulated data", *Journal of Engineering Mechanics*, vol. 130, no. 1, pp. 3–15, 2004. DOI: 10.1061/(ASCE)0733-9399(2004)130:1(3).

[23] L. Kalemba and S. H. Jakobsen, *Nordic 44 test newtork*, Sep. 2017.

[24] C. J.M., "Practical guidelines for the natural excitation technique (next) and the eigensystem realization algorithm (era) for modal identification using ambient vibration", *Experimental Techniques*, vol. 35, no. 4, pp. 52–58, DOI: 10.1111/j.1747-1567.2010.00643.x. eprint: https://onlinelibrary.wiley.com/doi/pdf/10.1111/j.1747-1567.2010.00643.x. [Online]. Available: https://onlinelibrary.wiley.com/doi/abs/10.1111/j.1747-1567.2010.00643.x.

Appendices

.1 Modification in Nordic 44

Figure 1 display the initial state 0f Nordic 44 model

```
---------------------------------------------------------------------------------------------------------------------------
| Load Flow Calculation                                                                                Total System Summary
---------------------------------------------------------------------------------------------------------------------------
|     AC Load Flow, balanced, positive sequence                |   Automatic Model Adaptation for Convergence            No
|     Automatic tap adjustment of transformers          No     |   Max. Acceptable Load Flow Error for
|     Consider reactive power limits                    No     |      Nodes                                           1,00 kVA
|                                                              |      Model Equations                                 0,10 %
---------------------------------------------------------------------------------------------------------------------------
---------------------------------------------------------------------------------------------------------------------------
| Total System Summary                                   | Study Case: Study Case                | Annex:                  / 1
---------------------------------------------------------------------------------------------------------------------------
|
| No. of Substations     3          No. of Busbars        50        No. of Terminals     36        No. of Lines          70
| No. of 2-w Trfs.       16         No. of 3-w Trfs.      0         No. of syn. Machines  20       No. of asyn.Machines  0
| No. of Loads           46         No. of Shunts/Filters 0         No. of SVS           0
|
| Generation            =   22423,73  MW         8530,04   Mvar    23991,36  MVA
| External Infeed       =       0,00  MW            0,00   Mvar        0,00  MVA
| Load P(U)             =   22335,00  MW        13128,48   Mvar    25907,71  MVA
| Load P(Un)            =   22335,00  MW        13128,48   Mvar    25907,71  MVA
| Load P(Un-U)          =      -0,00  MW            0,00   Mvar
| Motor Load            =       0,00  MW            0,00   Mvar        0,00  MVA
| Grid Losses           =      88,73  MW        -4598,43   Mvar
| Line Charging         =                       -5830,02   Mvar
| Compensation ind.     =                           0,00   Mvar
| Compensation cap.     =                           0,00   Mvar
|
| Installed Capacity    =   29045,45  MW
| Spinning Reserve      =    3998,68  MW
|
| Total Power Factor:
|   Generation          =        0,93  [-]
|   Load/Motor          =   0,86 / 0,00  [-]
|--------------------------------------------------------------------------------------------------------------------------
```

Figure 1: Summary of N44's initial state before it was modified

Figure 2 shows summary of Nordic 44 model state after it was modified.

Load Flow Calculation					Total System Summary
AC Load Flow, balanced, positive sequence			Automatic Model Adaptation for Convergence		No
Automatic tap adjustment of transformers		No	Max. Acceptable Load Flow Error for		
Consider reactive power limits		No	Nodes		1,00 kVA
			Model Equations		0,10 %

Total System Summary					Study Case: Study Case		Annex:	/ 1
No. of Substations	3	No. of Busbars	50	No. of Terminals	36	No. of Lines	70	
No. of 2-w Trfs.	16	No. of 3-w Trfs.	0	No. of syn. Machines	20	No. of asyn.Machines	0	
No. of Loads	46	No. of Shunts/Filters	0	No. of SVS	0			

Generation	=	22423,73	MW	8530,04	Mvar	23991,36 MVA
External Infeed	=	0,00	MW	0,00	Mvar	0,00 MVA
Load P(U)	=	22335,00	MW	13128,48	Mvar	25907,71 MVA
Load P(Un)	=	22335,00	MW	13128,48	Mvar	25907,71 MVA
Load P(Un-U)	=	-0,00	MW	0,00	Mvar	
Motor Load	=	0,00	MW	0,00	Mvar	0,00 MVA
Grid Losses	=	88,73	MW	-4598,43	Mvar	
Line Charging	=			-5830,02	Mvar	
Compensation ind.	=			0,00	Mvar	
Compensation cap.	=			0,00	Mvar	

Installed Capacity	=	29045,45	MW
Spinning Reserve	=	3998,68	MW

Total Power Factor:

Generation	=	0,93	[-]
Load/Motor	=	0,86 / 0,00	[-]

Figure 2: Summary of N44's post state after its modification

The table below shows the altered elements and the corresponding values that it was changed to.

Table 1: Modification in loads

	Original Model					Updated Model			
Terminal	Out of Service	Active Power[MW]	React.Power[MVAr]	App.Power [MVA]		Out of service	Active Power[MW]	React.Power[MVAr]	App.Power [MVA]
NORDLINK	0	-1190	0	1190	Changed to ->	1	-	-	-
NSN	0	-1400	0	1400	Changed to ->	1	-	-	-
OSLO2	0	922,019	200	943,4612	Changed to ->	0	2203,42	200	2212,47818
OSLO2	0	922,019	200	943,4612	Changed to ->	0	2203,42	200	2212,47818
OSLO1	0	667,235	100	674,687	Changed to ->	0	1149,77	100	1154,110503
KRISTIAN	0	391,638	125	411,1026	Changed to ->	0	674,86	125	686,3388519
KRISTIAN	0	391,638	125	411,1026	Changed to ->	0	674,86	125	686,3388519
NORDNED	0	-595	175	620,2016	Changed to ->	0	414	175	449,4674627
SKAGERAK	0	-1445	363	1489,897	Changed to ->	0	1412	363	1457,913921
BLAFALLI	0	696,245	400	802,9677	Changed to ->	0	1199,76	400	1264,683382
BLAFALLI	0	696,245	400	802,9677	Changed to ->	0	1199,76	400	1264,683382
SIMA	0	1253	-70	1254,954	Changed to ->	0	2651	-70	2651,924019
TRETTEN	0	482,962	70	488,0085	Changed to ->	0	1154,17	70	1156,290789
TRONDHEI	0	687,667	333	764,0516	Changed to ->	0	1013	333	1066,329217
TRONDHEI	0	687,667	333	764,0516	Changed to ->	0	1013	333	1066,329217
TRONDHEI	0	687,667	333	764,0516	Changed to ->	0	1013	333	1066,329217
TRONDHEI	1	-368	0	368	Changed to ->	1			0
ROSSAGA	0	1280	150	1288,759	Changed to ->	0	2489	150	2493,515791
GRUNDFOR	0	1365,088	648,616	1511,346	Changed to ->	0	2265	650	2356,422076
PORJUS	0	448,044	648,616	788,3186	Changed to ->	0	621	650	898,966629
HJALTA	0	448,044	109,766	461,2939	Changed to ->	0	621	110	630,6671071
DANNEBO_	0	504,923	614,689	795,4809	Changed to ->	0	1219	616	1365,802694
FORSMARK	0	717,973	565,793	914,1154	Changed to ->	0	1420,66	567	1529,628659
FORSMARK	0	717,973	565,793	914,1154	Changed to ->	0	1420,66	567	1529,628659
FORSMARK	0	717,973	565,793	914,1154	Changed to ->	0	1420,66	567	1529,628659
FORSMARK	1	-2500	0	2500	Changed to ->	1			0
OSKARSHA	0	615,23	399,149	733,3675	Changed to ->	0	1217,36	400	1281,391966
OSKARSHA	0	615,23	399,149	733,3675	Changed to ->	0	1217,36	400	1281,391966
RINGHALS	0	738,276	598,723	950,537	Changed to ->	0	1460,83	600	1579,248014
RINGHALS	0	738,276	598,723	950,537	Changed to ->	0	1460,83	600	1579,248014
RINGHALS	0	738,276	598,723	950,537	Changed to ->	0	1460,83	600	1579,248014
RINGHALS	0	738,276	598,723	950,537	Changed to ->	0	1460,83	600	1579,248014
STENKU_H	0	-1,996	261,442	261,4496	Changed to ->	0	-330	262	421,3597038
ARRIE_HV	0	150	10	150,333	Changed to ->	0	446	10	446,1120935
KARLSH_H	0	-1	0	1	Changed to ->	0	628	0	628
LT_HVDC	0	85	0	85	Changed to ->	0			0
MALMO	0	560,804	432,078	707,9495	Changed to ->	0	1240	433	1313,426435
MALMO	0	560,804	432,078	707,9495	Changed to ->	0	1240	433	1313,426435
MALMO	0	560,804	432,078	707,9495	Changed to ->	0	1240	433	1313,426435
OULU	0	859,446	209,739	884,6682	Changed to ->	0	1431,68	200	1445,582105
OULU	0	859,446	209,739	884,6682	Changed to ->	0	1431,68	200	1445,582105
OULU	1	-1728,478	0	1728,478	Changed to ->	1			0
ESTLINK_	0	209,739	-4,195	209,7809	Changed to ->	0	-1219	600	1358,661474
HELSINKI	0	956,602	73,409	959,4146	Changed to ->	0	1593,53	70	1595,066726
HELSINKI	0	956,602	73,409	959,4146	Changed to ->	0	1593,53	70	1595,066726
HELSINKI	0	956,602	73,409	959,4146	Changed to ->	0	1593,53	70	1595,066726
HELSINKI	0	956,602	73,409	959,4146	Changed to ->	0	1593,53	70	1595,066726
HELSINKI	0	956,602	73,409	959,4146	Changed to ->	0	1593,53	70	1595,066726
VYBORG_H	0	-530,639	629,216	823,0981	Changed to ->	0	343	-4	343,0233228